Quaternary International 644-645 (2023) 5–20

Contents lists available at ScienceDirect

Quaternary International

journal homepage: www.elsevier.com/locate/quaint

The middle to Late Holocene environment on the Iturup Island (Kurils, North Western Pacific)

Larisa Nazarova [a,b,c,*], Nadezhda G. Razjigaeva [d], Larisa A. Ganzey [d], Tatiana R. Makarova [d], Marina S. Lyashevskaya [d], Boris K. Biskaborn [b], Philipp Hoelzmann [e], Larisa V. Golovatyuk [f], Bernhard Diekmann [a,b]

[a] University of Potsdam, Institute of Earth and Environmental Sciences, 14476, Karl-Liebknecht-Str. 24-25, Potsdam-Golm, Germany
[b] Alfred Wegener Institute, Helmholtz Centre for Polar and Marine Research, Research Unit Potsdam, 14473, Telegrafenberg A43, Potsdam, Germany
[c] Kazan Federal University, 420018, Kremlyovskaya Str., 18, Kazan, Russia
[d] Pacific Geographical Institute FEB RAS, 690041, Radio St. 7, Vladivostok, Russia
[e] Freie Universität Berlin, Institut für Geographische Wissenschaften, 12249, Malteser Strasse 74-100, Berlin, Germany
[f] Samara Federal Research Scientific Center RAS, Institute of Ecology of Volga River Basin RAS, 445003, Togliatti, Komzina St., 10, Russia

ARTICLE INFO

Keywords:
Far East
Kuril islands
Palaeoclimate
Lake development
Vegetation history
Holocene

ABSTRACT

The Kuril Islands stretch southwest from Kamchatka, Russia, to Hokkaido, Japan and separate the Sea of Okhotsk from the northern Pacific Ocean. A series of transgressions and regressions linked to variations in climatically affected global ice volume are among the most important drivers of Holocene environmental changes in the region. Despite a long research history, reconstructions of the Holocene palaeoenvironment are sparse with inconsistent interpretations, arising from insufficient dating control, different temporal resolutions, and specific local geographical features, such as high tectonic activity and the isolated nature of the area. We have investigated a 550 cm lake sediment section from Iturup Island, the largest among the Kuril Islands. The 6600 year old sediment section was studied using sedimentological, geochemical, chironomid, diatom, and pollen analyses to reconstruct environmental and climatic changes and sea level fluctuations (transgression – regression stages). During the warm late phase of the Middle Holocene (6600–4400 cal BP) an open bay or lagoon with shallow overgrown littorals existed at the sampling site. The cooling between 5600 and 4400 cal BP can be correlated with Neoglacial cooling. The cool period between 4200 and 3200 cal BP was a transition towards the formation of a freshwater lagoon and can be related to a decline of the Japan Late Jomon transgression (Sakaguchi, 1983). Between 3200 and 2800 cal BP the lagoon separated from the marine environment in response to a further sea level decrease during the Japan Latest Jomon cold stage and regression. The following increase in the share of broad-leaved pollen indicated a slight warming (Yayoi transition stage) that was interrupted by a short-term cooling spell between 1500 and 1400 cal BP (cold Japan Kofun stage). The period between ca 1100 and 800 cal BP can be related to the European Medieval Climate Anomaly (MCA) or relatively dry Japan Nara-Heian-Kamakura warm stage. The Little Ice Age cooling and Edo regression were evident after ca 800 cal BP. Modern warming however is not well seen in the investigated core.

1. Introduction

The environmental history of the Holocene climate variability in North Eastern Asia have been intensively studied during the past decades (Hong et al., 2001, 2005; Seki et al., 2009; Zhou et al., 2010; Chu et al., 2014; Stebich et al., 2015; Jo et al., 2017; Zheng et al., 2018; Zhao et al., 2021). However, despite a long research history, reconstructions of Holocene palaeoenvironments and vegetation dynamic in marginal basin of the North Western Pacific (NWP), including Kamchatka Peninsula and Kuril Islands (Russian Far East) remain sparse with inconsistent interpretations arising from insufficient dating of paleorecords, differing temporal resolutions, and specific local geographical features (Krasheninnikov, 1949, (1755); Komarov, 1940; Razjigaeva et al., 2008, 2013, 2019b; Lozhkin et al., 2010, 2017; Nazarova et al.,

* Corresponding author. University of Potsdam, Institute of Earth and Environmental Sciences, 14476, Karl-Liebknecht-Str. 24, Potsdam-Golm, Germany.
E-mail address: Larisa.nazarova@awi.de (L. Nazarova).

https://doi.org/10.1016/j.quaint.2021.05.003
Received 22 February 2021; Received in revised form 7 May 2021; Accepted 7 May 2021
Available online 15 May 2021

2017a, 2019). The Kuril Islands (Fig. 1) that stretch southwest from Kamchatka, Russia, to Hokkaido, Japan separating the Sea of Okhotsk from the northern Pacific Ocean are unique and climatically an extremely sensitive region (Razjigaeva et al., 2011, 2013; Lozhkin et al., 2017) that remain among the most scarcely populated and least studied regions on Earth (Brooks et al., 2015; Nazarova et al., 2020). Due to their geographical position, Kuril Islands are strongly affected by the warming of the cryosphere in the Arctic and subarctic Pacific regions (Biskaborn et al., 2019a, b), by neighbouring landmasses of north-eastern Eurasia, and by several atmospheric teleconnections (Pacific Decadal

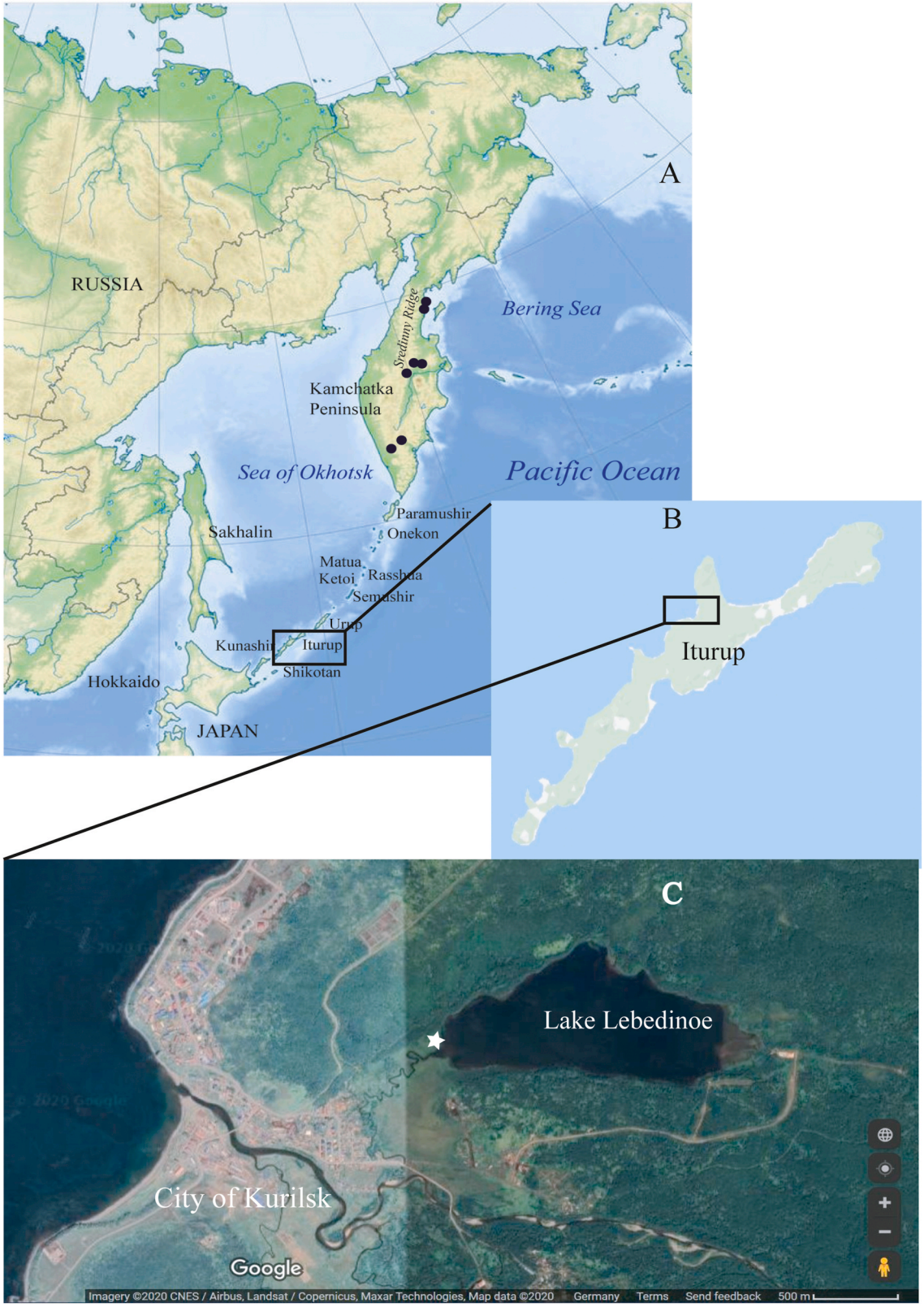

Fig. 1. A. Location of the Iturup Island; B. Location of the study area; C. Position of the sampling site.

Oscillation, El-Niño/Southern-Oscillation, Arctic Oscillation) (Saenko et al., 2004; Anderson et al., 2005; Melles et al., 2012; Nazarova et al., 2017b). Besides, the Kuril Islands are part of the ring of tectonic instability surrounding the Pacific Ocean (Ring of Fire). Neotectonic movements and sea level changes have played an important role in the evolution of the region during different intervals of the Holocene (Melekestsev et al., 1974; Razjigaeva et al., 2008; Anderson et al., 2015; Lozhkin et al., 2017). A series of transgressions and regressions linked to variations in climatically caused global ice volume are among the most important drivers of Holocene environmental changes in the coastal Far East mainland and NWP Islands (Korotky et al., 1997, 2000, 2000; Razjigaeva et al., 2002, 2004, 2016, 2004; Lozhkin et al., 2017). Another major factor influencing the environment in the region are the numerous ash falls from volcanoes that often locally overprint climatic signals (Razjigaeva et al., 2011; Razzhigaeva et al., 2016). Palaeovegetation dynamic is strongly influenced as well by the isolated nature of the area, impeding plant migration from the mainland of Siberia or from Japan Islands (Komarov, 1940). Evaluating the accuracy of the palaeoclimate and the sea-level history of the region is particularly challenging as well due to lack of continuous records of exposed marine and terrestrial sections (Lozhkin et al., 2017).

In this paper we present the results of sedimentological, geochemical, chironomid, diatom, and pollen analyses of newly obtained continuous Holocene deposits from Iturup Island, the largest among the Kuril Islands (Fig. 1). Earlier investigations of the landscape structure of the island together with palynological investigation of several sediment sections from the vicinity of the Kurilsk settlement (Fig. 1) have shown that palaeolandscape changes on Iturup Island in the Middle to Late Holocene were mainly determined by climatic fluctuations, as well as by sea level fluctuations, and volcanic eruptions (Razjigaeva et al., 2002; Lyashchevskaya and Ganzey, 2011). However, the poor age control of the investigated sections did not allow the identification of the timing of climatic and neotectonics events. A recent investigation of two lacustrine records from the Iturup Island were built on provisional age schemes. This study, though it couldn't confirm the timing of the environmental history of the region (Lozhkin et al., 2017), revealed several moot points. For example, palynological data from the Northern and Central Kuril Islands suggest that climate changes during the Middle to Late Holocene were minimal and/or gradual. However, similarly to the Southern Kurils (Razjigaeva et al., 2013), more fluctuating conditions were interpreted from the Iturup sections. Changes in geomorphology and diatom flora could be linked to sea-level oscillations caused by climatic warming and cooling, but the timing of these events remains unclear (Lozhkin et al., 2017).

The main aim of our study is to reconstruct the environmental and climatic changes on Iturup Island, Southern Kuriles, using a multi-proxy investigation of the sediment section from a swampy area at the shore of lake Lebedinoe, situated ca 1.5 km from the coast of the Kurilskiy bay of the Sea of Okhotsk (Fig. 1). The stratigraphic study of the sediment sequence focusses on environmental reconstruction in response to such factors as the regional climate and sea level fluctuations (transgression – regression stages). Our multiproxy study, and comparison of our newly obtained results with earlier published data from other Kuril Islands (Razjigaeva et al., 2008, 2011, 2013, 2019b, 2011, 2019b; Lozhkin et al., 2017), Japan (Sakaguchi, 1983) and other NE Asian records (Biskaborn et al., 2012, 2016; Brooks et al., 2015; Koizumi et al., 2006; Park et al., 2019; Zhao et al., 2021, etc.) provides new insights into the spatial variability of the palaeoclimate in this poorly studies area of the NWP.

2. Regional settings and sampling site

Iturup Island is the largest island of the Kuril island arc. It is elongated in a northeastern direction, with a length of 200 km and a width of 5.5–46 km. The island has a mountainous volcanic-tectonic relief, formed by several volcanic massifs and ridges connected by hilly and low-lying valleys. A series of calc-alkaline volcanoes form the NE to SW backbone of the island (Melekestsev et al., 1974; Laverov, 2005; Ganzey and Ivanov, 2012). The highest volcano Stokap (1634 m) is located in the central part of Iturup. There are several plateaus formed by outflows of basalts. The shoreline of the island is mostly high and steep (Lyashchevskaya and Ganzey, 2011).

The climate of the island is temperate monsoonal and is controlled by the Asiatic Low and the North Pacific High in summer, and by the Siberian High and Aleutian Low in winter (Martyn, 1992). A distinctive feature of the climate is the strong microclimatic variability related to the influence of relief, presence of hydrothermal springs, and the influence of sea currents (Kotlyakov et al., 2009). The microclimate of the island at the Sea of Okhotsk and the Pacific coasts differs significantly. On the side of the Sea of Okhotsk, the warm Soya Current passes by the island, whereas on the Pacific side, the cold Oyashio Current influences the island (Kotlyakov et al., 2009). According to the archive data from the last 10 years from the meteorological station Kurilsk, situated at the Iturup Island (http://www.pogodaiklimat.ru/history/32174.htm), the mean February air temperature (T^o) is −5.14°C, the mean July air T^o is 14.5 °C and the mean annual T^o is 5.45 °C. The mean annual precipitation for the last 10 years has been 1374 mm. The precipitation is unevenly distributed over the seasons, with maximum precipitation occurring in December (165 mm) and the lowest precipitation from February (89 mm) to May (79 mm). Winters on the island are much milder than on the continent and are characterised by frequent snowfalls and thaws. Frequent cyclones and typhoons that originate in the tropical zone pass through the islands bringing heavy rain- and snowfall. Strong NW winds (winds >15 m/s) prevail in autumn and winter, shifting to the SW and SE during summer (Ivanova, 1990; Ecology, 2002).

The vegetation on the island is diverse (Vorobiev, 1963; Urusov and Chipizubova, 2000; Barkalov, 2009). Dark coniferous and birch forests are present in the southern part of the island. Larch and birch forests occupy the central and northern parts. Sparse forests of larch and stone birch prevail on isthmuses and low-lying areas. Kuril bamboo (*Sasa* sp.) grows in the understory of stone-birch forests. Brush pine dominates the slopes above 700 m and the northern slopes are occupied by alder. Tall grasses are characteristic for river valleys. Meadow communities are widespread on the coastal lowlands and dunes, while swamps occupy the flattened areas around lakes (Lyashchevskaya and Ganzey, 2011).

In the NW part of the island, a vast lowland (2 × 1.5 km) occupies a former sea bay at the top of the Kuril Gulf in the lower reaches of the Kurilka river (Fig. 1). The lowland has a rather complex structure due to the formation of coastal barriers of different ages and the migration of the Kurilka river and its tributaries (Razjigaeva et al., 2002; Lyashchevskaya and Ganzey, 2011). Lake Lebedinoe (LL) is situated ca 1.5 km from the coast of the Sea of Okhotsk. The LL has a lagoonal origin and is located within the inner part of the coastal lowland in the mouth of a small stream, a tributary of the Kurilka river. The LL is 1930 m in length, 840 m wide, with a maximal depth of 3 m, and is situated at an elevation of 1 m asl.

3. Material and methods

3.1. Coring, age model, lithology, organic, and inorganic geochemistry

Field work on the Iturup Island took place in the summer of 2009. A sediment core was obtained from a swampy area located on the Kuril Bay coast 1450 m from the shoreline and 80 m from the coast of Lake Lebedinoe (45°13.874′N, 147°53.442′E (45.23151, 147.8907); Fig. 1) using a Hiller peat-borer. The obtained 550 cm sediment core (field #6409) was split in the laboratory into 3–5 cm thick intervals, resulting in 113 samples (Supplementary Electronic Material (SEM), Table 1). Geochemical and chironomid analysis was performed on all samples. Diatom and pollen analyses were performed on 59 samples: every sample from the depths 0–18 cm, and every second sample from the rest of the core (depth 18–550 cm, resolution 3–5 cm).

Sediment samples were dated in the AMS Laboratory at Taiwan University (samples with laboratory ID NTUAMS) and in the Laboratory of the Geological Institute, Russian Academy of Science, Moscow (samples with laboratory ID MU) (SEM, Table 2). To model the age-depth relationship we applied the Bacon 2.2 package (Blaauw and Christen, 2011) for R software (R Core Team, 2012) and the IntCal20 calibration curve (Reimer et al., 2020) (Fig. 2).

Total organic carbon (TOC) and nitrogen (N) of freeze-dried and milled samples were analysed using a Vario EL III CNS and a Vario MAX C analyser. The measurement accuracy was 0.1 wt % for TOC and total nitrogen (TN), and 0.05 wt % for total carbon (TC) (Fig. 3).

A portable energy-dispersive X-ray fluorescence spectrometer (P-ED XRF) Analyticon NITON XL3t was used for elemental analyses. Approximately 4 g of the grinded, dried, and homogenised samples were placed in plastic cups and sealed with mylar foil (0.4 μm). The prepared sample-cups were placed on the P-EDXRF and measured for 120 s with different filters to detect specific elements (SEM, Table 3).

Only elements that showed mean values larger than four times the 2 sigma error of the measurements (Al, Ca, Cl, Fe, K, P, Rb, S, Si, Sr, Ti, Zr) were taken into account for the analyses (Schwanghart et al., 2016). Constant measurement conditions were checked by analysing a certified reference material (CRM) after every tenth sample measurement. Soil (NCS DC 73387; NCS DC73389; Anonymous, 2008) and lake sediment LKSD-2 (Lynch, 1990) were used as CRMs, producing recovery values between 87.8% and 111,1% for most of the elements (SEM, Table 4).

3.2. Diatom analysis

Diatom slide preparation followed standard methods using the water-bath technique (Battarbee, 1986). Diatom slides were mounted using Elyashev aniline-formaldehyde resin with refraction indices of 1.66–1.68 (Gleser et al., 1974), identified and counted (no less than 300 valves per sample) under an Axioplan Zeiss light microscope equipped with an oil-immersion objective. Diatoms were identified to the highest possible taxonomic resolution following mainly Krammer and Lange-Bertalot (1986, 1991), in accordance with modern taxonomy as given in the AlgaeBase database with the latest revisions (Genkal et al., 2013; Guiry and Guiry, 2019; AlgaeBase). The total number of valves was taken as 100% of which we defined taxa with abundances ≥10% and ≥5% as dominants and subdominants, respectively (Palagushkina et al., 2012). The ecological characteristics of indicator species with respect to preferences of habitat, pH, water salinity, as well as changes in the ice cover duration and the spring/autumn turbulence period were described following Davydova (1985), Van Dam et al. (1994), Fallu et al. (2000), Barinova et al. (2006) (Figs. 4 and 5).

3.3. Chironomid analysis

The treatment of sediment samples for chironomid analysis followed standard techniques described in Brooks et al. (2007). Larval head capsules were mounted in Hydromatrix. Chironomids remains have been found in 57 of 113 samples but more than 50 head capsules (HC) – which is necessary for a reliable quantitative reconstruction (Larocque, 2001; Heiri and Lotter, 2001; Quinlan and Smol, 2001) – were found in only 11 of them. To capture the higher diversity of the chironomid communities in order to increase the reliability of qualitative palaeoecological estimations we compiled the investigated samples with low concentrations of the HC together and extrapolated the sum of the

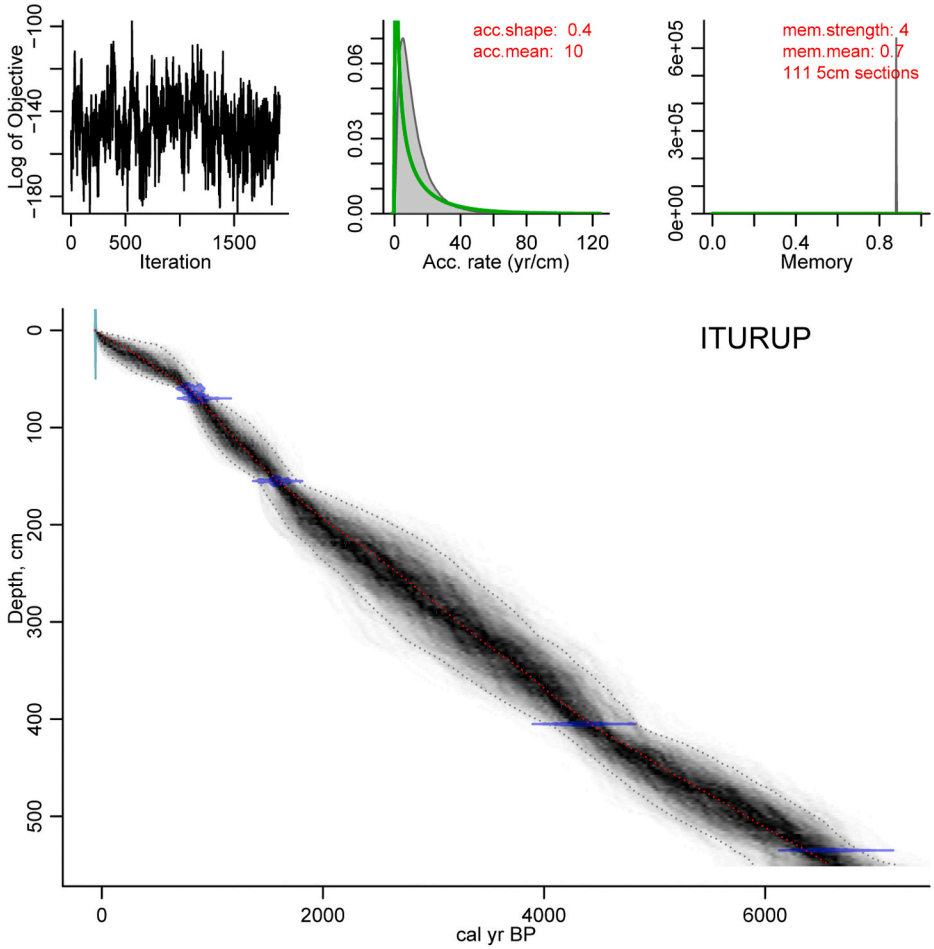

Fig. 2. Age-depth model for the sediments of the palaeolake (#6409).

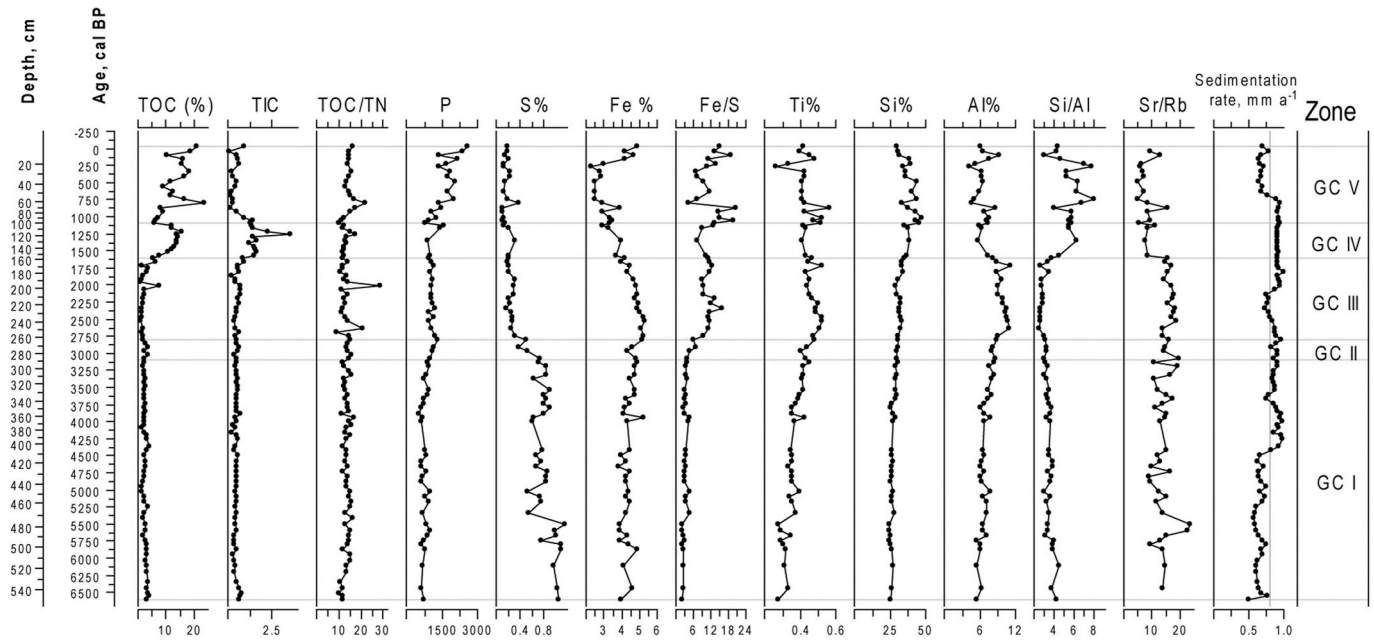

Fig. 3. Organic and inorganic geochemical composition of the sediment core from the palaeolake (#6409). TOC, TIC, and TN were determined by elementary analyses and are given in wt. %, while TOC/TN was calculated as atomic ratio. Al, Fe, P, S, Si, Rb, Sr, and Ti were analysed using p-ED-XRF; their concentrations are given in percent (%) or parts per million (ppm).

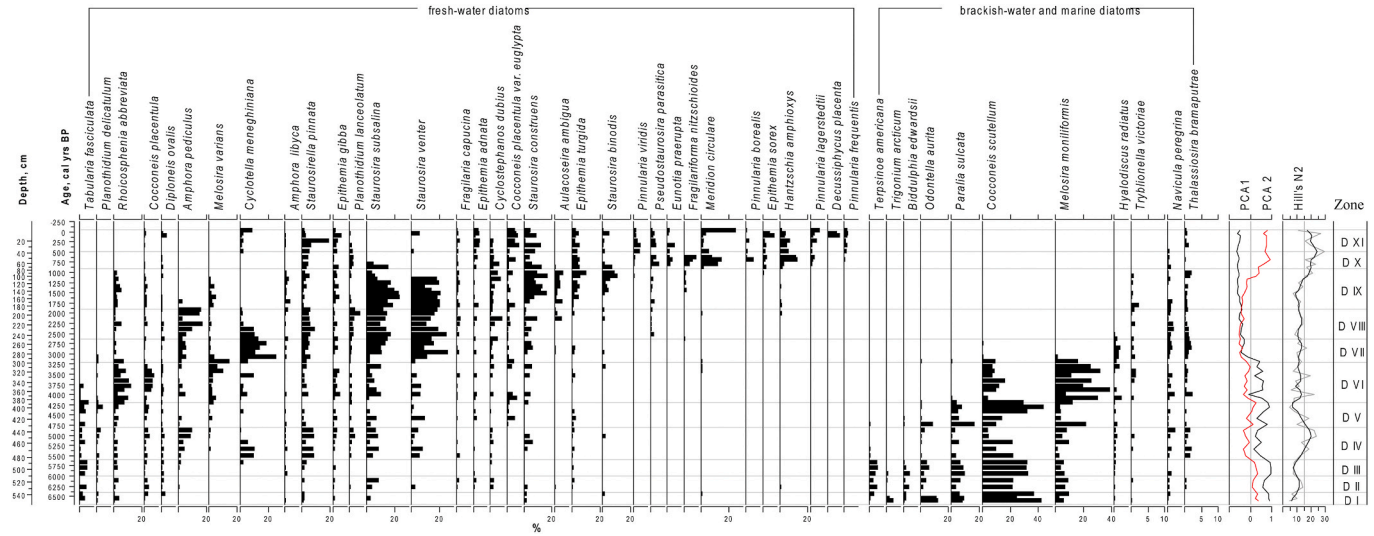

Fig. 4. Stratigraphic diagram showing the distribution of the main diatom taxa in sediment core from the palaeolake (#6409, Iturup Island), PCA axes 1 and 2 scores for diatom data, and Hill's N2 diversity.

samples onto the median depth of the compiled samples. In the end we obtained 31 chironomid samples. Parts of the core where no chironomid HC were found are marked in grey on the stratigraphic diagram (Fig. 6). Chironomids were identified to the highest taxonomic resolution with reference to Wiederholm (1983) and Brooks et al. (2007). Information on the ecology of chironomid taxa was obtained from Brooks et al. (2007), Moller Pilot (2009, 2013) and Nazarova et al. (2008, 2011, 2015; 2017a, c), and values of T July and WD optima of chironomids were obtained from Nazarova et al. (2008, 2011, 2015).

3.4. Pollen analysis

Samples for pollen analysis were treated with a potassium cadmium heavy liquid (2.2 g per cm^3) (Pokrovskaya, 1966). At least 300 pollen grains and spores were counted in saturated samples. The identification of the pollen and spores was performed using pollen atlases (Kuprianova and Alyoshina, 1972; Reille, 1992, 1995, 1998). Percentages of all taxa were calculated based on setting the total of all pollen and spore taxa to equal 100%. The quantitative relationship was determined between three main groups of taxa: tree and shrub pollen (AP); herbs and grass together with low shrub (NAP); and spores (Fig. 7).

3.5. Data analysis

Stratigraphic diagrams were created in C2 version 1.5 (Juggins, 2007). Zonation was done using the optimal sum-of-squares partitioning method (Birks and Gordon, 1985) using the program ZONE (Lotter and Juggins, 1991). The number of significant zones was assessed with a broken stick model (Bennett, 1996) using BSTICK (Birks and Line, unpublished). The effective numbers of occurrences of chironomid,

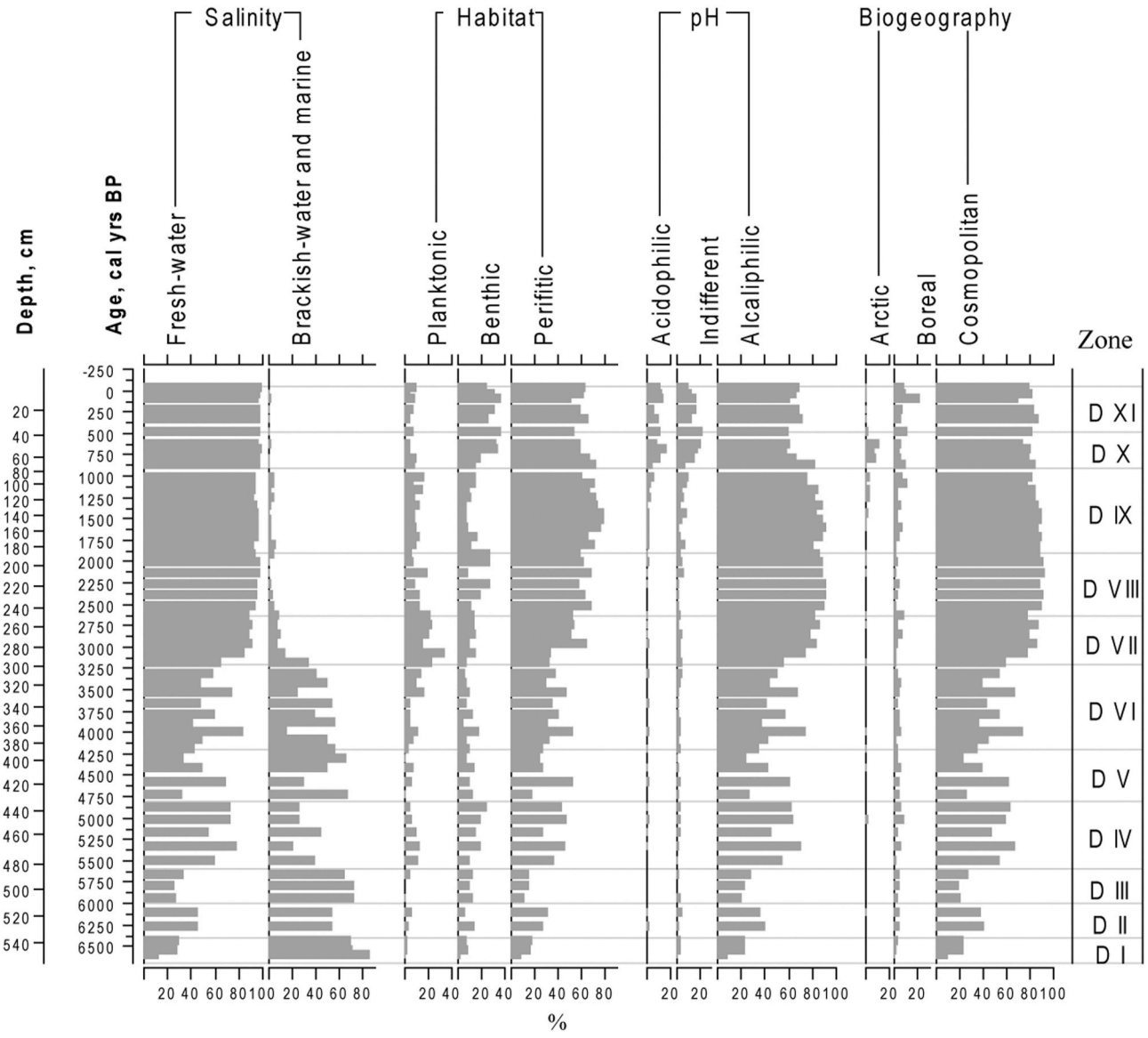

Fig. 5. Distribution of ecological groups of diatoms in sediments of the palaeolake (#6409) from the Iturup Island with regard to salinity, habitat type, pH, and geographical distribution.

diatom, and pollen taxa were estimated using the N2 index (Hill, 1973). Principal Component Analysis (PCA) was used to explore the main pattern of taxonomic variations of chironomids, diatoms, and pollen data throughout the sediment core (ter Braak and Prentice, 1988; Solovieva et al., 2015) and as additional proof of zonation. PCA were performed using CANOCO 4.5 (ter Braak and Šmilauer, 2002). Species percentage data were square root transformed, and rare taxa were downweighted.

4. Results

4.1. Age model, lithology, and geochemistry

The lower part of the section (SEM, Table 1) is composed of non-layered pelitic silt. Individual interlayers are enriched with small fragments of thin-walled shells of molluscs. The interval between 290 and 180 cm is composed of greenish-grey silted sand with a layer of silt at the base of the interval and brown fine-grained silted sand in the upper part. Between 180 and 68 cm the core consists of an olive-grey and brown gyttja with inclusions of wood remains. The upper part of the core (68–0 cm) is composed of peat with layers of gyttja and peaty silt.

The 14C results show that the dates are in chronological order (Fig. 2 and SEM, Table 2). The obtained dates span the last ca 6600 years. The applied age model suggests that sedimentation rates varied between 0.5 mm a^{-1} (113 cm; 6600 cal BP) and 0.99 mm a^{-1} (178 cm; 1810 cal BP) averaging at 0.81 mm a^{-1}.

4.2. Geochemical (p-ED-XRF) analyses

The p-ED-XRF spectrometer analyses (n = 73) produced reliable measurements for a total of 13 elements (Al, Ca, Cl, Fe, K, Mn, P, Rb, S, Sr, Ti, Rb, Zr; cf. Fig. 3; SEM, Table 4). We focus on the concentrations of the single elements Al, Fe, P, S, Si, and Ti, as well as the element mole ratios of Fe/S, Si/Al, and Sr/Rb as these reflect changes within the marine-lagoon-lake system in terms of productivity (P, TOC), and marine (S; Berner and Raiswell, 1984; Chambers et al., 2000; Chéron et al., 2016) vs terrestrial (Fe) influence. Si/Al ratios illustrate changes in detrital input and opal (Pleskot et al., 2018; Vyse et al., 2020), the latter being regarded as presenting higher diatom concentrations. Sr/Rb ratios represent changes in grain size (Koinig et al., 2003; Heinecke et al.,

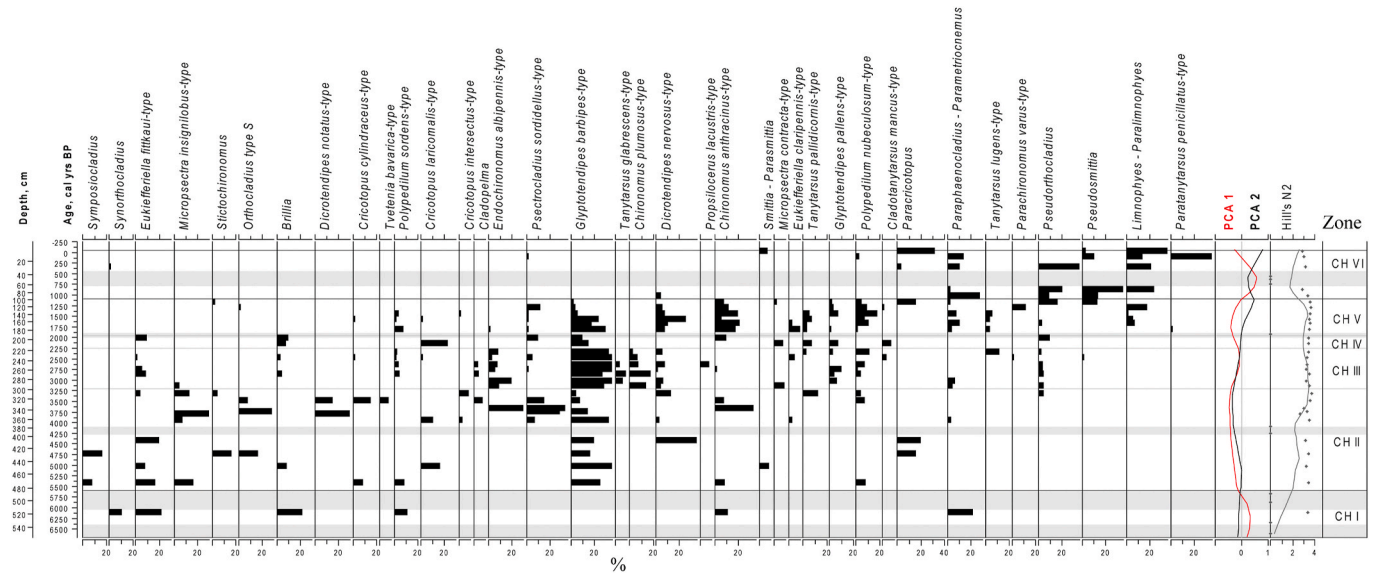

Fig. 6. Relative proportions of the most abundant chironomid taxa in the sediments of the palaeolake (#6409) from the Iturup Island, PCA axes 1 and 2 scores for chironomid data, Hill's N2 diversity. For N2 black dots represent the data and the grey line represents a LOESS 0.2 smoothing of the data. The grey horizontal intervals represent parts of the core where no chironomids have been found.

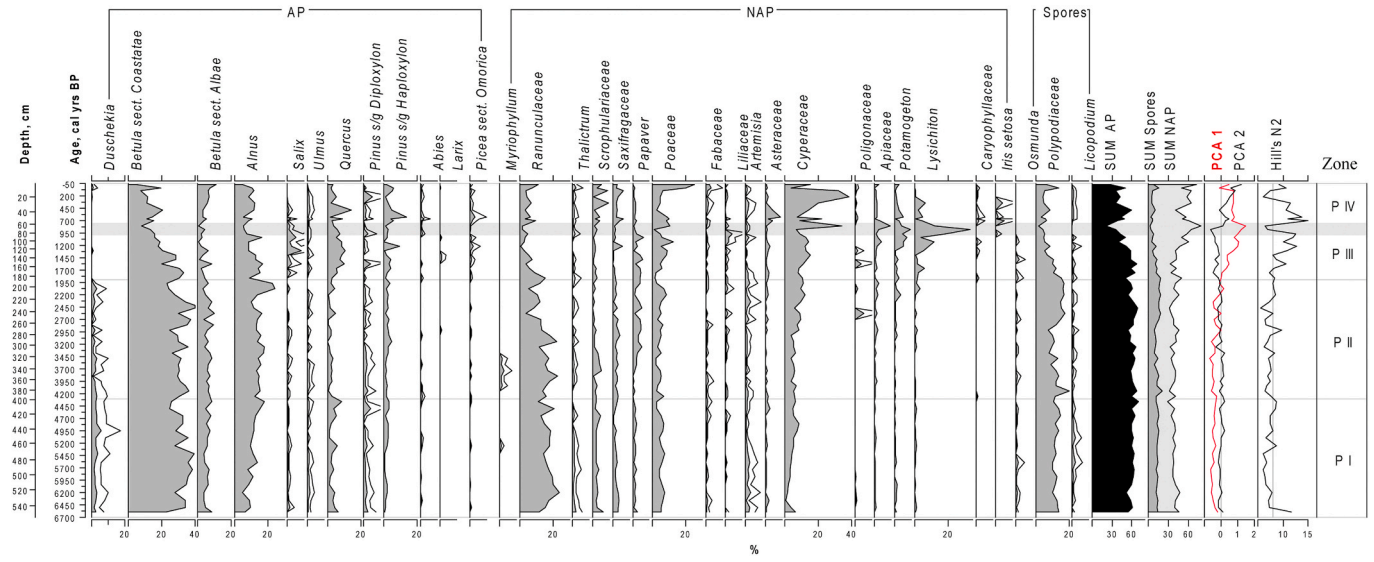

Fig. 7. Stratigraphic diagram showing the distribution of the main pollen taxa in the sediment core from the palaeolake (#6409, Iturup Island), PCA axes 1 and 2 scores for pollen data, and Hill's N2 diversity.

2017) that are strongly related to the mineral composition of the supply material (Biskaborn et al., 2019).

GC I (560–288 cm; 6600–3100 cal BP). This section is characterised by low TOC values between 1.3 and 3.9% and the lowest P contents (<0.1% P). Sulphur exhibits high values between 0.5 to 1.2% with the highest values around 1% S between 6600 and 5500 cal BP. Although relatively high values of Fe (around 4%) are observed, the Fe/S ratios remain low (<4.8) due to the high S content. The Al and Ti values run parallel to each other with low values that increase slightly. Si exhibits low values that increase slightly and therefore the Si/Al ratios remain on a similar level throughout this zone. High Sr/Rb ratios are seen with fluctuations between 6000 and 5000 cal BP.

GC II (288–258 cm; 3100–2700 cal BP). Within this section the sulphur decreases to values below 0.5% S whereas P, Fe, Al, and Ti show increasing values. Consequently, the Fe/S ratio increases from 4.6 to 9.4. The Si/Al ratio remains constant as both elements show slight but parallel increases.

GC III (258–168 cm; 2700–1700 cal BP). Within this part of the core the sulphur values stabilise to a relatively low level (~0.25 %S) like P (0.1% P). Si (32%), Ti (0.48%), Fe (4.9%), and Al (10%) show no major variations within the unit or in the underlying unit. Since Si and Al run parallel, no changes are seen in the Si/Al ratio. The Fe/S ratio exhibit values around 11.5 which are substantially above those of all underlying units.

GC IV (168–103 cm; 1700–1100 cal BP). This section is characterised by a strong increase of TOC to average values above 11.6% and reflects TOC/TN ratios between 11 and 17. The TIC values also increase from below 1% to a sharp peak at 118 cm with 3.6% TIC. The other elements (S, P, Fe, Ti, Al) maintain similar values as in the underlying unit except for Sr, which shows a decrease at 153 cm and consequently the Sr/Rb ratio also drops from values of around 15 to 9.

GC V (105–0 cm; 1100 – -50 cal BP). Some elements such as Si, Al,

Ti, and Fe show relatively strong changes throughout this unit, but the latter is nonetheless characterised by high TOC (up to 23.5% TOC) and TOC/TN ratios of around 15. From 100 cm upwards, P shows increasing values that are highest at the top of the core (0.26% P), whereas sulphur shows the lowest values of the core within this unit. Iron exhibits values around 3.3% Fe which are highest in the top 16 cm of the core (4.5%). Consequently, the Fe/S ratio reflects the iron concentrations and points to high values at the top of the core. Si and Ti show stronger variations than Al for which the values decrease towards the top, leading to an increased Si/Al ratio for this unit.

4.3. Diatom analysis

We have identified 167 species of freshwater and 52 species of brackish-water and marine diatoms in the studied core. The diversity of diatom complexes remained low (median N2 = 11.1) until ca 5800 cal BP and rose thereafter, reaching a maximum (23–24) between ca 5000 and 4800 cal BP. Diatom diversity subsequently declined to the lowest value of 4.7 at 4300 cal BP and fluctuated between 8 and 13 until ca 1500 cal BP. After ca 1500 cal BP the diversity of diatoms had a steady increasing trend with the highest N2 = 29 at ca 490 cal BP, after which diversity declined again towards the surface of the sample.

We have identified 11 diatom complexes that are reflected by variations of PCA 1 and 2 samples scores (Figs. 4 and 5).

D I (560–545 cm; 6600–6400 cal BP) is characterised by the predominance of marine and brackish-water diatoms (up to 86.4%). Benthic species prevail (up to 47.1%). The proportion of planktonic species reaches up to 31.2%. The dominating species include brackish-water benthic *Cocconeis scutellum* (up to 42%), *Rhabdonema arcuatum* (up to 4.5%), euryhaline *Melosira moniliformis* (up to 10%), *Tabularia fasciculata*, marine planktonic *Odontella aurita* (up to 12%), *Paralia sulcata* (up to 9%), and neritic *Triceratum arctium* (up to 5%). Among periphytic freshwater diatoms we found inhabitants of slightly brackish waters (*Rhoicosphenia abbreviata*, *Rhopalodia gibba*, R. *gibberula*) and *Staurosira construens*, *S. subsalina*, S. *venter*, and *Staurosirella pinnata* which are common in lakes that are shallow and overgrown by macrophytes.

D II (545–515 cm; 6400–6000 cal BP) is characterised by a decrease in the marine and brackish-water diatoms (from 86 to 54%). Planktonic species decline to 14.5%. Benthic *Cocconeis scutellum* decreases and the euryhaline littoral-planktonic *Melosira moniliformis*, brackish-water *Terpsinoe Americana*, *Diplonies interrupta*, and planktonic brackish-freshwater *Thalassiosira bramaputrae* increase. Among freshwater diatoms, the abundance of peryphitic *Staurosirella pinnata, Staurosira construens*, *S. subsalina*, and *Cocconeis placentula* which are usual in lakes and slow-flowing waters increase. Planktonic *Cyclostephanos dubius* which is characteristic of lakes also appears.

D 3 (515–505 cm; 6000–5600 cal BP). The abundance of marine and brackish-water diatoms increases to 73%. Benthic species dominate. The most abundant are *Cocconeis scutellum* (up to 33%), *Melosira moniliformis* (up to 7%), and *Terpsinoe americana* (up to 6%). The share of planktonic species increases to 24%, with dominating *Paralia sulcata* (up to 10%) and *Odontella aurita* (up to 6%). *Staurosira construens, S. subsalina,* and *S. venter* disappear from freshwater diatoms, and the euryhaline *Tabularia fasciculata* and *Planothidium delicatulum* slightly increase.

D IV (505–445 cm; 5600–4800 cal BP). The share of marine and brackish-water diatoms decreases and fluctuates within 45–20%. Benthic and euryhaline *Melosira moniliformis* increases (up to 10%). *Thalassiosira bramaputrae, Tryblionella littoralis,* and *T. victoriae*, which are typical for estuaries and lagoons, become more common. The abundance of planktonic species does not exceed 9%. Among freshwater diatoms, the share of lotic diatoms, characteristic for riverine ecosystems diatoms, including planktonic *Cyclotella meneghiniana* (up to 10.5%), benthic *Amphora pediculus* (up to 10%) and periphytic *Staurosira subsalina* (up to 9%) and *Staurosirella pinnata* (up to 9%) increase.

D V (445–395 cm; 4800–4200 cal ys BP). The abundance of marine and brackish-water diatoms varies between 50 and 67% and only decreases to 30% at the depth of 425 cm (4580 cal BP). Benthic species dominate (up to 56.2%). Euryhaline *Melosira moniliformis* dominates in the lower and upper layers of this sediment interval (up to 30%). In the middle part the *Cocconeis scutellum* becomes more abundant (up to 44%). The share of planktonic diatoms remains low (no more than 10%) and only at the depths of 425 cm (4580 cal BP) reaches 30.2%, where *Paralia sulcata* is found in higher abundances. Freshwater diatoms are represented by species that are characteristic of stagnant and slowly flowing waters: planktonic *Melosira varians*, periphytic *Rhoicosphenia abbreviata*, *Rhopalodia gibberula, Surirella tenera,* and *Cocconeis placentula* var. *Euglypta*.

D VI (395–315 cm; 4200–3200 cal ys BP) is characterised by a gradual decrease in the abundance of and significant taxonomic changes of brackish-water and marine diatoms. The abundance of planktonic diatoms decreases (2.0–7.2%). The euryhaline benthic *Melosira moniliformis* increase (up to 38.8%). Between 335 and 350 cm (3500–3700 cal BP) *Cocconeis scutellum* increase up to 16.4%. Freshwater diatoms are dominated by planktonic *Melosira varians* (up to 15%), *Cyclotella meneghiniana* (up to 10%), and periphytic *Rhoicosphenia abbreviata* (up to 12.5%), characteristic of oligotrophic-mesotrophic water bodies of riverine systems.

DVII (315–255 cm; 3200–2600 cal BP). Brackish-water and marine diatoms strongly decline. Among the benthic species, the most frequently occurring species are those inhabiting highly desalinated lagoons and estuaries (*Thalassiosira bramaputrae*, *Tryblionella littoralis*, *T. victoriae*, and *T. apiculate*). The complex of dominant freshwater diatoms includes planktonic *Cyclotella meneghiniana* (up to 25.6%), periphytic *Staurosira venter* (up to 26%), *Staurosira subsalina* (up to 15%), *S. construens, Staurosirella pinnata*, and benthic *Amphora pediculus*.

D VIII (255–195 cm; 2600–1900 cal BP). Marine and brackish diatoms further decline (up to 1.6–5.6%). The dominant species of freshwater diatoms are largely similar to that of the previous zone. However, a slight decrease in the proportion of planktonic species and an increase in benthic diatoms (up to 28.6%) are observed. Among them *Amphora pediculus* reaches abundances of up to 17.6%. Alkaliphilic species dominate with respect to pH, and indifferent diatoms dominate with respect to salinity. Brackish-water diatoms *Thalassiosira bramaputrae* and *Tryblionella victoriae* are constantly present in sediments. Small amounts of marine planktonic diatoms *Thalassiosira kryophila* and *Paralia sulcate* can be transported into the lake through the connecting channel during storm surges.

D IX (195–95 cm; 1900–900 cal BP). Freshwater diatoms dominate this complex (93.8–97.9%), among which periphytic species reach up to 80%. Among planktonic diatoms, *Cyclostephanos dubius, Melosira varians*, and various species of the genus *Aulacoseira* increase (up to 17.5%). Benthic diatoms decrease. Brackish-water diatoms are represented by *Thalassiosira bramaputrae* (up to 2.3%) and *Tryblionella victoriae*. In the upper part of the core (after 120 cm; 1100 cal BP), the abundance of arctoboreal (up to 4.1%) and boreal species (up to 12.4%) increase.

D X (95–40 cm; 900–485 cal BP). Periphytic species *Staurosira subsalina, S. venter*, and *Meridion circulare* characteristic of flowing waters, dominate. The abundance of planktonic species decreases whilst the proportion of halophobic species increases. Cosmopolitan species dominate but the abundance of arctoboreal (up to 17%) and boreal (up to 23%) species increase. Brackish-water diatoms *Thalassiosira bramaputrae*, *Tryblionella plana,* and *T. littoralis* occur occasionally, but most are probably transported by storm surges.

D XI (40–0 cm; 485 – -50 cal BP). Periphytic species characteristic of different types of water bodies substantially prevail. The most frequent are *Cocconeis placentula* var. *Euglypta, Epithemia adnata, E. turgida, E. sorex,* and *Staurosira construens.* In the upper sediment layers planktonic *Cyclotella meneghiniana* increase. The abundance of acidophilic diatoms reaches 14.5%, including *Decussata placenta* (benthic, characteristic of shallow lakes). At the surface of the sample, *Meridion*

circulare, characteristic of flowing waters, significantly increases (up to 25%). Single occurrences of several brackish-water and marine diatoms (*Thalassiosira bramaputrae, Coscinodiscus marginatus, Actinocyclus octonarius,* and *Paralia sulcate*) can most likely be associated with strong storm surges.

4.4. Chironomid analysis

In total we have identified 62 chironomid taxa in the investigated core, 11 of which only had a single occurrence. Chironomid communities were very scarce, with N2 diversity slightly varying between 2.6 at 3800 cal BP and 3.7 at 3300 cal BP, averaging at 3.3 (Fig. 6). Several intervals didn't contain chironomid remains at all (marked in grey in Fig. 6). Six zones (CH I–VI) were revealed, based on down-core changes in the chironomid assemblages (Fig. 6).

CH I (560–505 cm; 6600–5600 cal BP). In this interval chironomids were found only at the depth of 525 cm (6100 cal BP). The chironomid community is very scarce and consists only of 6 taxa (N2 = 3.4). Four of them occur mainly in flowing waters: *Synorthocladius*, *Eukiefferiella fittkaui*-type, *Brillia,* and *Paraphaenocladius-Parametriocnemus*. The *Polypedilum sordens*-type is a phytophilic taxon and *Chironomus anthracinus*-type is a eurytopic taxon that can be among the early colonisers of the new environments or the environments with sub-optimal conditions.

CH II (505–315 cm; 5600–3200 cal BP). After 5600 cal BP the diversity of chironomid communities rises. Taxa characteristic of lotic conditions (*E. fittkaui*-type, *Brillia, Paracricotopus*) remain abundant until 4300 cal BP. During this interval, the lotic fauna is supplemented by *Symposiocladius*, a running waters wood miner which is rarely found in lake sediments. After 5600 cal BP *Glyptotendipes barbipes*-type appear in the communities and remain abundant until 1200 cal BP with some decline at 3200 cal BP. This taxon occurs in detritus-rich meso-to eutrophic lakes and is a miner of macrophytes. It is reported to be found in high abundances at salinities up to 3‰, and at lower numbers at even higher salinities (Cannings and Scudder, 1978). The species richness of phytophilic fauna rises and includes different taxa from the genus *Cricotopus* and *P. sordens*-type. Between 4300 and 4200 cal BP, no chironomids were found in the sediments. However, the tendency of increasing richness of phytophilic fauna also remains after 4200 cal BP. *Micropsectra insignilobus*-type, *Dicrotendipes notatus*-type and *Dicrotendipes nervosus*-type, *Polypedilum nubeculosum*-type, *Endochironomus albipennis*-type groups, etc., appear in the lake. Between 3900 and 3300 cal BP the *Psectrocladius sordidellus*-type species has the highest abundances. The taxon is characteristic of temperate conditions, occurring in littoral regions and often dominating acidified lakes. In the studied lake it has the highest abundance in line with rises of *C. anthracinus*-type and *E. albipennis*-type and the decline of brackish-water tolerant *G. barbipes*-type.

CH III (315–225 cm; 3200–2200 cal BP). This interval is dominated by *G. barbipes*-type and several other lentic phitophilic taxa characteristic of meso-to euthrophic conditions (*C. anthracinus*-type, *E. albipennis*-type, *P. nubeculosum*-type). Some lotic taxa are found sporadically (*Brillia, E. fittkaui*-type). *Pseudorthocladius*, which is common in very shallow waters, springs, and the splash zones of lakes is constantly present in small abundances.

CH IV (225–195 cm; 2200–1900 cal BP). This short interval is characterised by a strong decline of *G. barbipes*-type, as well as an increase of lotic taxa (*Brillia, E. fittkaui*-type*, Pseudorthocladius*), phytophilic *Cricotopus laricomalis*-type, and acidophilic *P. sordidellus*-type.

CH V (195–105 cm; 1950–1100 cal BP). Lotic taxa disappear from the lake and chironomid assemblages are dominated by typical for lentic meso-euthrophic conditions in presence of macrophytes taxa: *C. anthracinus*-type, *D. nervosus*-type, and *P. nubeculosum*-type. *G. barbipes*-type decline and disappear from the chironomid communities after 1200 cal BP. At 1200 cal BP, there is an increase in *P. sordidellus*-type and *Paracricotopus* that is mainly attributed to mosses and small streams.

CH VI (105–0 cm; 1100 – -50 cal BP). The fauna is dominated by mainly semiterrestrial taxa or taxa characteristic of very shallow waters, springs, splash zones of lakes, or mosses: *Paraphaenocladius-Parametriocnemus, Pseudosmittia*, *Pseudorthocladius,* and *Limnophies-Paralimnophies*, that reach their highest abundances at ca 900 cal BP. Between 800 and 450 cal BP no chironomids were found, but the fauna after 450 cal BP consists of the taxa from the same ecological group as before 800 cal BP but is enriched by very low abundances of phytophilic *P. nubeculosum*-type, *P. sordidellus*-type and a strong increase in the abundances of phytophilic *Paratanytarsus penicillatus*-type typical of moderate conditions.

4.5. Pollen analysis

A total of 106 different pollen, and spore types have been identified. The pollen stratigraphic diagram is subdivided into four pollen zones (P I-IV) (Fig. 7).

P I (560–400 cm; 6600–4300 cal BP). Arboreal pollen (AP) predominates. Birch pollen dominates, especially *Betula* sect. *Costatae* (up to 38.7%), the source of which is the stone birch *Betula ermanii*. A variety of broad-leaved pollen was noted (up to 11.3%), including *Quercus, Ulmus,* and *Acer*. Coniferous pollen (*Abies, Picea*) was found in small quantities. An abundance of *Alnus* increases towards the top of the zone (up to 17.8%). *Duschekia* increases up to 5.8% between 5000 and 4800 cal BP. Ranunculaceae, typical of the vegetation of valleys and lake shores, are the most abundant among non-arboreal pollen (NAP) types. The pollen of aquatic plants (*Potamogeton, Sparganium, Nuphar, Myriophyllum*) is only found in low quantities. Among spores, ferns (Polypodiaceae, *Osmunda*) predominate. *Sphagnum* is found in small quantities.

P II (400–195 cm; 4300–1900 cal BP). The abundance of the *Betula* pollen increases (up to 44.3%), and pollen of broad-leaved trees decrease (up to 6.5%). A particularly low content of broad-leaved pollen (1.3–2.1%) was noted between 2800 and 2650 cal BP. The proportion of alder pollen significantly increases (up to 24%), especially between 2100 and 2000 cal BP. After ca 3000 cal BP, Ranunculaceae decrease and *Cyperaceae* increase.

P III (195–65 cm; 1900–750 cal BP). There is a trend towards an increase in NAP pollen (up to 76.6%) and broad-leaved pollen (up to 12.2%), especially *Quercus* (up to 10.8%). The proportion of *Betula* pollen is reduced. *Larix* appear between 1500 and 1400 cal BP. At ca 1200 cal BP, *Salix* willows spread around the lake reaching their highest abundance of 8.6% and the dwarf *Pinus* s/g *Haploxylon* increase up to 9.3%. In the NAP group, the proportion of pollen from plants typical of marshes (*Cyperaceae*, *Lysichiton*) and wet meadows (Apiaceae) increases. From 1200 cal BP, aquatic pollen increase, especially *Potamogeton*, which is characteristic of shallow freshwater bodies. The pollen of Ranunculaceae, which are mainly transported with river water, decrease significantly. At ca 900 cal BP a significant increase of *Cyperaceae* and *Lysichiton*, and a strong decline in pollen taxonomic diversity are observed.

P IV (65–0 cm; 750 – -50 cal BP) corresponds to the modern vegetation in the study area. NAP pollen predominates, indicating the development of grass communities on the lowland. Dwarf pines increase significantly at ca 760 cal BP. Broad-leaved pollen decreases after ca 400 cal BP. Pollen of *Cyperaceae* sedges increase up to 38.3% and *Alnus* pollen also increases. Shrubs began to develop and Scrophulariaceae become widely represented. In the modern samples their number decreases, and Poaceae become dominant (up to 25%).

5. Discussion

The changes in the lithology, geochemistry, the fossil diatom, chironomid and pollen assemblages, and their interpretation with respect to the ecological spectra of species revealed several stages in the development of the studied "lagoon-lake" system and in the

palaeoclimate on Iturup Island during the Middle to Late Holocene. In the discussion we relate the reconstructed palaeoclimatic fluctuations on Iturup Island to the data from the other Kuril Islands, to the Japan climatic stages correlated with the documented ancient history of Japan (Sakaguchi, 1983) and to the wide known middle to late Holocene climatic events (Fig. 8).

5.1. Middle Holocene (6600-4400 cal BP)

Chironomids, that are known to inhabit only fresh- or slightly brackish-water environments, are mainly absent or seldom present in the lower part of the core. Marine and brackish-water diatoms have the highest concentrations (Figs. 4, 5 and 8) and freshwater diatoms are represented by species that can withstand slightly brackish conditions or species that are typical of shallow lakes and lakes overgrown by macrophytes (*S. construens*, *S. subsalina*, S. *venter*, *Staurosirella pinnata*). Active sea surges are evident from the periodic appearance of oceanic north-boreal diatom species (*Coscinodiscus marginatus, C. oculus-iridis, Thalassiosira eccentrica*; not in Fig. 4). This diatom complex could develop in an open bay or lagoon with shallow overgrown littorals under a strong marine influence. The latter is also reflected in the highest contents of sulphur in sediments that originated primarily from marine waters (Chambers et al., 2000). Since iron is deposited from terrestrial sources, the Fe/S ratio (Figs. 3 and 8) can be used to geochemically differentiate between the terrestrial and marine influences where low ratios point to more marine or lagoonal phases, whereas enriched Fe/S ratios reflect increasing freshwater conditions (Chagué-Goff et al., 2012; Hoelzmann et al., 2017). Although the Fe contents are relatively high, the Fe/S ratios reflect the lowest values and a strong marine influence, corroborated by low organic carbon and low phosphorus contents, both representing low nutrient supply during this marine-lagoonal phase. Also, terrestrial detrital input is low as shown by the low Si, Ti, and Al contents.

The vegetation on the island corresponded to a warm mixed forest (Gotanda et al., 2002). Pollen of *Pinus* s/g *Diploxylon* and *Cryptomeria* were probably transferred to the region from Hokkaido (Razjigaeva et al., 2008). These taxa were previously found in modern pollen rain on Kunashir Island, Southern Kuriles (Fig. 8) (Mokhova and Eremenko, 2020).

This period of this relatively warm conditions and high sea level corresponds to the second part of the Holocene climatic optimum (HCO), which is well represented across continental Siberia and the Far East (Nazarova et al., 2013a, b; Biskaborn et al., 2012, 2016). The climax of the HCO occurred at similar time on the neighbouring smaller islands of Southern Kuriles: on Shikotan Island it appeared around 6400 to 5300 cal BP (Razjigaeva et al., 2008; Nazarova et al., 2017b) and on the Kunashir between ca 6500 and 5000 cal BP (Korotky et al., 2000). In the south of Shikotan (Fig. 1), the high abundances of diatom species characteristic of soils in peat sections (Razjigaeva et al., 2008) indicate decreased moisture availability during this period caused by both the reduced annual precipitation and enhanced evaporation due to the increased active temperatures.

On Japanese Islands HCO is equivalent to the Early Jomon warmest stage and transgression that took place between ca 8400 to 5200 cal BP (Fig. 8) with some short-term climatic deteriorations and low amplitude regressions (Sakaguchi, 1983). This stage in the northern and eastern Japanese Islands was characterised by a warmer climate than at present (Sakaguchi, 1983).

Natural processes in the region were controlled both by global climatic changes and by the migration of warm and cold marine currents (Korotky et al., 2000). The Tsushima Current, flowing off Japan at this time (ca 6700-5500 cal BP), reached northern Hokkaido as far north as

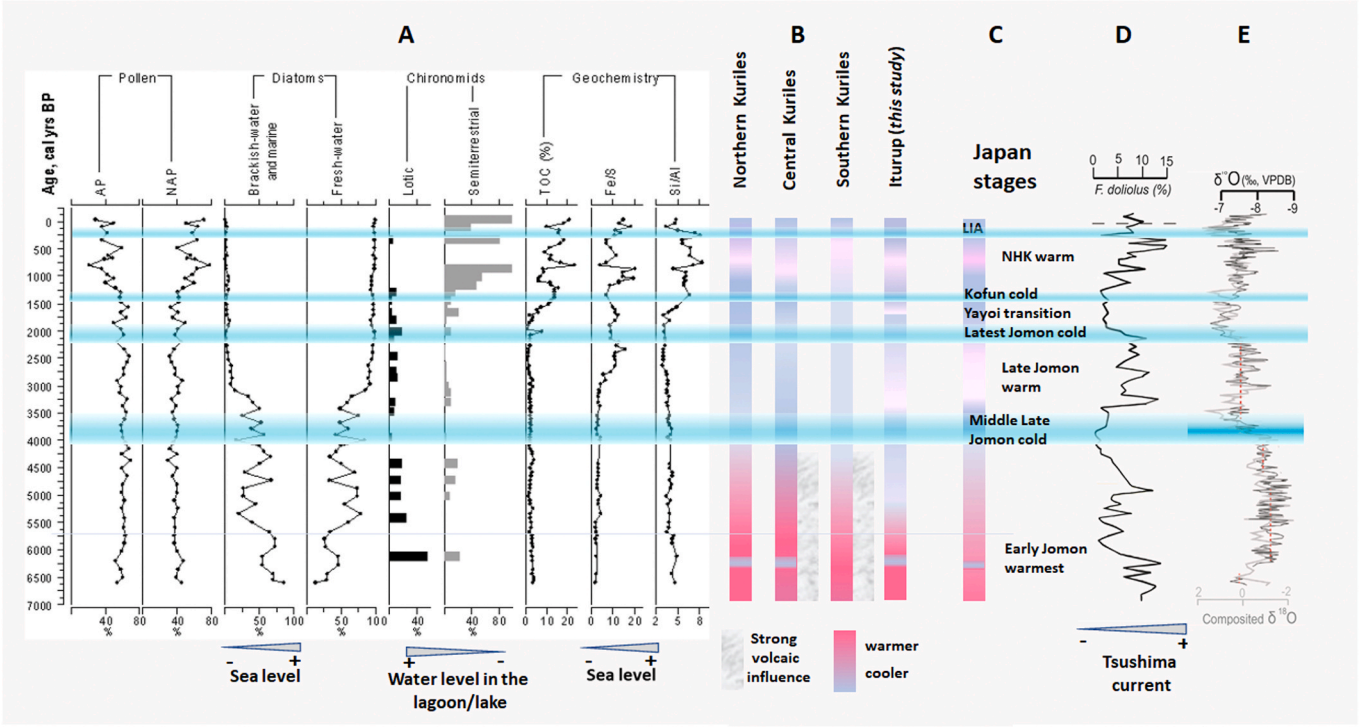

Fig. 8. Compilation of palaeoenvironmental interpretations for the Middle to Late Holocene: (A) relative abundancies of the selected proxies from the investigated palaeolake (#6409) record, Iturup Island, Southern Kuriles; (B) Temperature trends for Southern, Central and Northern Kuril Islands (Razjigaeva et al., 2008, 2011, 2013) and inferred from palaeolake (#6409) record, climatic trends in the Iturup Island, southern Kuriles. (C) Japan climatic stages (after Sakaguchi, 1983); (D) Abundance of warm diatom species *F. doliolus* in oceanic sediment from Oki Ridge (Japan; core D-GC-6), reflecting Tsushima warm current intensity (Koizumi et al., 2006). (E) Speleothem record from Liu-li (LL) cave, northeastern China: d18O record (black) and composite d18O record (grey) Horizontal red lines depict mean d18O values for each period (Zhao et al., 2021). The horizontal blue bar shows the abrupt Monsoon declines (Wang et al., 2006). (For interpretation of the references to colour in this figure legend, the reader is referred to the Web version of this article.)

45°N (Taira, 1980, 1992, 1992; Taira and Lutaenko, 1993; Koizumi et al., 2006). The sea-level rise of up to 2.5–3 m above present sea level (PSL) (Sakaguchi, 1983; Korotky and Khudyakov, 1990; Maeda et al., 1994; Sato et al., 1998; Kaplin and Selivanov, 1999; Korotky et al., 1997, 2005). This Holocene transgression led to a full disconnection of the Southern Kurils from Hokkaido (Kulakov, 1973; Sakaguchi, 1983; Sakaguchi and Okumura, 1986; Korotky et al., 2000; Razjigaeva et al., 2008) and to the development of lagoons at the study site on Iturup Island as well as in other low laying bays of the Kuril Islands (Korotky et al., 2000; Lozhkin et al., 2017; Nazarova et al., 2017b, 2018). Mean annual temperatures on the Kuril Islands were probably 2–3 °C higher than modern ones, especially in the Southern Kurils (Razjigaeva et al., 2002). This is indicated by widespread mixed coniferous-broadleaf forests and cool-temperate broadleaf forests on the Kunashir, Iturup, and Shikotan islands that may spread up to Urup Island (northernmost island of the Southern Kuriles, 45°54′ E, 149°59′N; Korotky et al., 2000; Razjigaeva et al., 2002, 2004, 2008, 2019b; Lyaschevskaya and Ganzei, 2011).

Though prominent in Southern Kuriles, the HCO warming was less pronounced on Central and Northern Kuril Islands than in other regions of the Far East (Korotky et al., 2000, 2005, 2005; Velichko, 2010; Brooks et al., 2015). In the Central and Northern Kurils the HCO is not well pronounced, probably because of strong volcanic activity (Razjigaeva et al., 2011; Nakagawa et al., 2008) (Fig. 8). A strong eruption at Tao-Rusyr ca 7500 B P (ca 8350 cal BP; Melekestsev et al., 1974; Laverov, 2005) and other local volcanoes had a severe impact on the surrounding islands. Shrubs were widespread only in areas where volcanic activity was insignificant, e.g., in the south of Paramushir Island (Northern Kuriles; Fig. 8) where dwarf pines and alder became more widespread.

However, during the late phase of the HCO (6600-4400 cal BP) in the investigated record from Iturup Island, considerable variations in diatom diversity, shifts in dominating taxa, and the sporadic emergence of freshwater chironomids (Fig. 8) suggest unstable ecological conditions and changes in water level related to sea level changes and probably, to the intensity of the run-off with the inflowing river. These changes are reflected as well through varying sulphur and iron contents as well as fluctuations in grain sizes reflected by Sr/Rb ratios between 5800 and 4900 cal BP (Fig. 3).

The dominating during the Middle Holocene marine benthic *Cocconeis scutellum* (Fig. 4) declined between 6300 and 6100 cal BP and between 5600 and 4400 cal BP. During these intervals, the concentrations and diversity of freshwater diatoms increased, and freshwater chironomids appeared in the lagoon, indicating decreasing salinity and lower sea level. The taxonomically poor chironomid community consisted mainly of the taxa present in flowing waters (*Synorthocladius*, *Eukiefferiella fittkaui*-type, *Brillia, Paraphaenocladius-Parametriocnemus*) that would most likely have been transported to the site with the inflowing river. Ranunculaceae, typical for the vegetation of valleys, lakes, and rivers shores, increased in the pollen spectra, supporting the desalinisation of the brackish-water lagoon related to the weakening of the connection with the sea or the increase of run-off with the inflowing river.

The decline of marine diatoms between 6300 and 6100 cal BP alongside with appearance of freshwater chironomids, short-term decline of *Betula*, and rise of Duscheckia can be related to a weak cooling that occurred ca 6500 to 6200 cal BP and a slight regression that was traced in Japan, on Kunashir, and some other islands at 5700–5400 B P (6450-6200 cal BP) (Sakaguchi, 1983).

The following decline of marine diatoms between 5600 and 4400 cal BP was accompanied by the reappearance of freshwater chironomids in the sediments. Chironomid communities during this interval were dominated by brackish-water tolerant *G. barbipes*-type (Cannings and Scudder, 1978). This suggest that the fresh-to slightly brackish-water chironomid communities could develop “on-site” and only some lotic taxa could be transported with the tributary river. Increasing C/N ratios (Fig. 3) indicate higher bioproductivity in the catchment area and the rising input of allochthonous carbon between 5500 and 4950 cal BP (Biskaborn et al., 2012, 2016; Meyers and Teranes, 2001). In the geochemical data this can be seen from the decline of sulphur contents at 5500 cal BP reflecting a decreasing marine influence. All these changes indicate the weakening of the connections between the lagoon and the ocean and provide evidence for another regression and related salinity decrease in the lagoon which is further supported by the gradual increase of *Cyperaceae* around 4950 cal BP and a peak in the abundance of *Duschekia*, which require sufficient soil humidity. Regression and associated coarsening grain size are evidenced by a peak in Sr/Rb ratios around 5600 cal BP.

These findings are in accordance with the most significant regression of sea level in the Middle to Late Holocene which relates to cooling dated after ca 5450 cal BP on Kunashir Island (4700–4500 B P, Korotky et al., 2000) and at 5500-5100 cal BP on Shikotan Island (Nazarova et al., 2017b). The sea level is estimated to have been 4–5 m below the PSL (Korotky and Khudyakov, 1990). This regression can be correlated with the Middle Jomon regression and Middle/Late Jomon cold stage (Ota et al., 1982; Sakaguchi, 1983) which were reconstructed in Japanese Islands between 5100 and 4700 cal BP (5000-4000 B P) and with the Neoglacial cooling that has been registered in other sites across the NWP, in various Eurasian and North American regions (Meyer et al., 2015; Solovieva et al., 2015; Syrykh et al., 2017). In Hokkaido and in South Kurils vegetation changed only slightly, possibly because of the influence of warm currents (Igarashi and Kumano, 1974; Tsukada, 1986; Korotky et al., 2000; Lozhkin et al., 2010; Razjigaeva et al., 2011). In the Central Kurils local volcanoes were semi-active and Neoglacial cooling did not influence significantly islands flora and fauna. In Rasshua Island (Fig. 1) the areas occupied by birch decreased. In north Kuril Islands cooling had little impact. However, increases in sea-ice extent in the Okhotsk and Bering Seas (Harada et al., 2014) after ca 4500 cal BP indicated the impact of the Neoglacial cooling. In the mainland of the Far East and in Sakhalin Island it was accompanied by decreasing precipitation (Khotinsky, 1977; Mikishin and Gvozdeva, 1996; Korotky et al., 2005).

This cooling is usually related to one of the major weakening of the Asian Monsoon (4.5–4.0 ka BP event; Wang et al., 2005) that alongside with the 8.2 ka BP event has longer duration and larger magnitude. This event has been reported in various other localities in Asia (Dixit et al., 2014; Park et al., 2019; Zhao et al., 2021). In the Holocene Dongge record this abrupt lowering of Asian Monsoon intensity is recorded over several decades (Wang et al., 2005) and reflects strongly enhanced aridity in western China (Wu et al., 2004), Korea (Park et al., 2019) and is in phase with the Mesopotamian dry event in western Asia (deMenocal, 2001).

5.2. Late Holocene (4400 cal BP - to present)

Between 4400 and 4200 cal BP, a prominent rise in the concentration of marine diatoms indicates the strengthening of the marine influence on the lagoon (marine transgression) and amelioration of the climate. During this interval chironomids disappeared from the sediments most probably in response to a rise in water salinity. In the vegetation, *Betula* declines. A slight increase in *Quercus* and *Alnus* populations supports the prevalence of warm conditions. This period corresponds to the first Late Jomon warm stage and transgression (ca 4700 to 3400 cal BP; Sakaguchi, 1983) with a sea-level rise of approximately 1.2–2.5 m above PSL.

The period between 4200 and 3200 cal BP was characterised by a strong shift in ecological groups of diatoms (Fig. 8). Earlier dominating marine benthic *Cocconeis scutellum* was replaced by the brackish water/euryhaline benthic *Melosira moniliformis* (Fig. 4) which generally indicates the lower salinity of the lagoon. However, active sea surges and a sea level corresponding to a transgression stage are evident from the remanent presence of relatively high abundances of the former dominant *Cocconeis scutellum,* neritic *Hyalodiscus radiatus*, and arctoboreal

Thalassiosira kryophila (Fig. 4). In general, increasing share of freshwater diatom species (Fig. 8) indicates a transition towards the formation of a freshwater lagoon. The freshwater diatoms were dominated by planktonic (*Melosira varians, Cyclotella meneghiniana),* and periphytic (*Rhoicosphenia abbreviate)* species characteristic of oligotrophic-mesotrophic water bodies with riverine influences. Within this phase the Si, Al, and P values slightly increase (Fig. 3) and point to increasing detrital (Si, Al) and nutrient (P) input under stronger riverine influence and/or decreasing marine influence, also reflected in rising Fe/S ratios (Fig. 8).

The diversity of chironomid communities rose (Fig. 6). Brackish-water tolerant *G. barbipes*-type taxa declined towards 3200 cal BP, in line with the rise in species richness of freshwater phytophilic fauna typical of stagnant waters (*Cricotopus*, *P. sordens-type*. *Micropsectra insignilobus*-type, *Dicrotendipes notatus*-type and *D. nervosus*-type, *Polypedilum nubeculosum*-type, *Endochironomus albipennis*-type, etc.). During this period *Myriophyllum* was widespread in the lagoon. These submersed aquatic plants grow best in still waters and thrive in areas with a light sandy bottom and medium loamy soils at depths of 50–200 cm (Gubanov et al., 2013).

The composition of aquatic biological communities indicates that between 4200 and 3200 cal BP the salinity of the lagoon decreased, freshwater flora and fauna replaced brackish-water resistant taxa, and under moderately warm conditions, a shallow water stagnant lagoon overgrown by macrophytes was formed. At 3100 cal BP the main decrease of S (Chéron et al., 2016) and rise in TOC and TC began, indicating a transition from an open lagoon to a closed fresh-water lake. This period can be related to a decline of the Late Jomon transgression (Sakaguchi, 1983).

After 3200 cal BP brackish-water and marine diatoms were found in small abundances only. This is in accordance with the steady decrease of S and the increasing Fe/S ratio between 3200 and 2800 cal BP indicating the successive closure of the lake system and thus, its separation from the marine environment. Between 3200 and 1900 cal BP, chironomids were present and communities were dominated by lentic phytophilic taxa characteristic of meso-to euthrophic conditions in the presence of some lotic taxa. In pollen spectra after ca 3000 cal BP the concentrations of *Cyperaceae* grew. All these indicate the formation of a freshwater shallow lake completely separated from the ocean and suggest a further sea level decrease.

A short interval between 2200 and 1900 cal BP characterised by a strong decline of lentic chironomid taxa and increase of lotic taxa (*Brillia, E. fittkaui-type, Pseudorthocladius*), and phytophilic *Cricotopus laricomalis*-type taxa indicates an increase in water flow from the tributary river. The proportion of alder pollen significantly increased (Fig. 7), especially between 2100 and 2000 cal BP, which together with a decrease in the proportion of birch pollen at this interval, probably reflects cool and humid conditions.

At this time broadleaf and coniferous-broadleaf forests in the Southern Kurils decreased, and dark coniferous and birch forests became widely distributed. This cooling in the Central and North Kurils (Fig. 8) was indicated by the occurrence of tundra landscapes. The combination of dwarf stone pine with *Selaginella selaginoides* in pollen assemblages indicated abundant snowfalls (Heusser and Igarashi, 1994). Volcanic eruptions were more frequent and during the last 2600 years, the amount of exotic, wind-blow taxa increased in the Kuril Islands, indicating strong southerly winds (Razjigaeva et al., 2013).

This short period can correspond to the Latest Jomon cold stage in Japan (Sakaguchi, 1983) and climatic deterioration in Korea (Ahn and Hwang, 2015; Park et al., 2019). The temperature in Japan was estimated to be 2–3 °C below modern temperatures and the climate was associated with an increase in winter precipitation (Sakaguchi, 1983; Yasuda, 1995).

Between 1900 and 1200 cal BP an increase of planktonic and periphytic diatoms indicates a subsequent increase in lake water levels. Lotic chironomid taxa disappeared from the lake and the communities were dominated by the taxa typical of lentic meso-euthrophic conditions in the presence of macrophytes (*C. anthracinus*-type, *D. nervosus*-type, *P. nubeculosum*-type). An increase in the share of broad-leaved pollen, especially *Quercus*, indicates a slight warming that can represent Yayoi transition stage (2400-1600 cal BP; Sakaguchi, 1983) (Fig. 8). The main decrease in Sr/Rb ratios at about 1600 cal BP in parallel to slight eutrophication and acidification trends, indicates less detrital input. The increase in TOC at the same time (Fig. 8) indicates enhanced productivity and a more stable (vegetated) catchment, possibly associated to the supply of organic acids. Advanced soil development and decreased weathering of less exposed minerals in the catchment likely caused a decreased base cation supply as also reflected by the decrease of Al that caused an increase in the Si/Al ratios (Biskaborn et al., 2012). Increased TIC during this time may have resulted from the growth of a carbonate lake or terrestrial organisms (i.e., carbonate mollusc shells).

The appearance of *Larix* and *Betula* between 1500 and 1400 cal BP may reflect a short cooling spell that can be related to a cold Kofun stage in Japan (ca 1600-1300 cal BP; Sakaguchi, 1983). During the Japan cold Kofun stage (Sakaguchi, 1983) the cold Oyashio current had a stronger impact in the region, which led to an increase in rainfall, fogs, and strong winds, especially in the Southern Kurils (Razjigaeva et al., 2004). High moisture availability is reflected by the higher proportion of pollen from plants typical of marshes (*Cyperaceae*, *Lysichiton*) and wet meadows (Apiaceae) and by the dominance of chironomid taxa, mainly attributed to submerged vegetation (*P. sordidellus*-type and *Paracricotopus*).

Between 1100 and 800 cal BP the sum of NAP strongly increased with high proportions of *Cyperaceae* and *Lysichiton*, and the diversity of pollen decreased. Both *Cyperaceae* and *Lysichiton* are semi aquatic plants and can withstand weakly acidic water pH. *Lysichiton* prefer sunny to half-shady conditions on wet loamy soils with pH between 5 and 6.5 (Alberternst and Nawrath, 2002). The abundance of diatom planktonic species decreased after 1000 cal BP and in parallel, TOC/TN ratios constantly rose reaching a distinct peak value at 800 cal BP, indicating a shift towards a terrestrial organic matter origin and decreasing water levels (Schleusner et al., 2014). The semi-terrestrial chironomid taxa characteristic of very shallow waters, springs, splash zones of lakes, or mosses (*Paraphaenocladius-Parametriocnemus, Pseudosmittia*, *Pseudorthocladius, Limnophies-Paralimnophies*) reached their highest abundances at ca 900 cal BP, and disappeared until 450 cal BP. The lake probably began to shoal, shrink in size, and the surrounding area began to turn into a swamp. A rise in the abundances of the acidophilic diatom species from the genera *Eunotia* and *Pinnularia*, characteristic of marshy environments (up to 20% in sum) supports this assumption. Lower lake levels are also reflected in the high Si and higher Si/Al ratios. At this time, oak forests with birches, maple, and elm were widespread around the lake (Razjigaeva et al., 2002) suggesting the amelioration of the climatic conditions.

This warm phase of the lake shallowing and desiccation can be related to the European Medieval Climate Anomaly (MCA) or Japan Nara-Heian-Kamakura warm stage in Japan (1200-700 cal BP; Sakaguchi, 1983) (Fig. 8) that was characterised by warmer winters and summers, and decreased precipitation. The MCA was weakly pronounced on the Kuril Islands. However, some shifts in vegetation have been observed in the Southern Kurils. Oak and broad-leaf taxa appeared on Kunashir Island. Fir dominated the vegetation of Shikotan Island (Razjigaeva et al., 2008, 2019a, 2019a). In the north of Urup Island birch forests became common. The sum of active temperatures possibly exceeded modern ones by only 150–180 °C. In the south of the continental Far East the average temperature deviation from modern time may have been ca 1 °C (Korotky et al., 2005; Velichko, 2010).

After 800 cal BP NAP pollen predominated, indicating the development of grass communities on the coast. Dwarf pines increased significantly at ca 760 cal BP. This plant became widespread during the Little Ice Age (LIA) (Razjigaeva et al., 2002, 2013). Colder conditions are indicated by a decrease in broad-leaved pollen (Fig. 7). At this time, the lake area decreased, and swamps occupied the former lake shores, which is reflected by the increase in the pollen content of *Cyperaceae* sedges (up

to 38.3%). Scrophulariaceae became widely represented in grassy meadows and humid habitats. Increased sedimentary phosphorus (P) during that time can reflect either changes in the consumption of lake organisms and/or increased animal activity (husbandry?) and associated P sources in the catchment.

After ca 450 cal BP the chironomids reappeared in the lake. The fauna was composed of semi-terrestrial taxa typical of very shallow waters, springs, splash zones of lakes, or mosses, indicating swampy conditions. The periphytic diatom species prevailed substantially. The abundancees of benthic diatoms from the genus Pinnularia, that are characteristic of floodplain sediments, remained high. Among them *Pinnularia lagerstedtii* is an indicator of rather dry environments. The area became boggy, and the abundance of acidophilic diatoms reached 14.5%. Single occurrences of several brackish-water and marine diatoms can most likely be associated with strong storm surges.

The LIA was pronounced in the region. It was accompanied by an Edo regression (650-50 cal BP; Sakaguchi, 1983) that played an important role in the formation of the modern landscapes in the Southern Kurils (Korotky et al., 2000; Razjigaeva et al., 2011). The cooling was enhanced by a southward shift of warm marine currents and intensified the influence of the cold Oyashio current (Koizumi, 1994; Kawahata et al., 2003). In Japan, mean annual temperatures decreased by 1–2 °C and precipitation increased (Taira, 1980; Sakaguchi, 1983; Kitagawa and Matsumoto, 1995). On Kunashir Island temperatures were ca 2 °C lower than modern (Demezhko and Solomina, 2009). In the Southern Kurils the LIA cooling led to a decrease in broadleaf vegetation, the disappearance of oak on Shikotan Island, and the spread of dark coniferous and birch forests. The LIA in the Central Kurils was characterised by an increase in effective moisture, thickness of snow cover, and intensification of peat accumulation (Razjigaeva et al., 2013).

Modern warming is not well recorded in the investigated core. There is a slight signal in the uppermost part of the sample showing increased *Cyclotella meneghiniana* which can be related to stratification, potentially because of warming, and *Meridion circulare* indicative of riverine activity. The dominance of Poaceae in the modern samples may reflect anthropogenic changes in landscapes (drainage of marshes, laying of roads, etc.).

On Iturup Island and on all Kuril Islands in the NWP region Late Holocene climate was characterised by a short-term oscillation of cooling and warming events and related low-amplitude regression/transgression stages (Razjigaeva et al., 2011; Brooks et al., 2015). The documented in the studied sediments from the Iturup Island series of Late Holocene cold/dry events (Fig. 8) most probably can be related (within dating errors) to climatic events known in many monsoon regions and centered approximately at 4.2, 2.7, and 1.4 ka BP, 1400–1850 CE (Wang et al., 2005) that can be linked with Bond events primarily identified from the Northern Atlantic (Bond et al., 1997). Some of these events supposed to have a broader spatial extent than it was previously recognized (Wang et al., 2014) which proves the presence of teleconnections between the North Atlantic and North Pacific, that modulate climatic oscillations on a global scale. However, the environmental shifts in Kuril Islands and in the whole NWP region are not of similar magnitude and have more complex spatial and temporal patterns (Brooks et al., 2015; Nazarova et al., 2020). These differences are the result of the Holocene transgressions; microclimatic relief variability in the islands; disruptive volcanic activity and still are not fully understood (Korotky et al., 2000; Razjigaeva et al., 2004, 2011, 2013, 2019 a, b; Anderson et al., 2005, 2015; Lozhkin et al., 2010, 2017; Nazarova et al., 2017b, 2019). The Kuril Islands represent the northern edge of the East Asian monsoon and are strongly influenced by a complex of regional and extraregional factors (e.g., sea ice shifts, sea-surface temperatures in the North Pacific, oceanic currents). More additional well dated records are still needed for better understanding of the multiple mechanisms and feedbacks driving the climatic and environmental changes in this interesting and still scarcely investigated area of northeast Asia.

6. Conclusions

Our investigation of the well dated sediment section of a coastal palaeolake/lagoon from the Iturup Island, performed by geochemical, diatoms, chironomid, and pollen analyses suggests a lagoonal ecosystem that was subjected to both marine and terrestrial influences and responded sensitively to fluctuating climatic conditions, providing valuable information for reconstructing the regional palaeoclimatic history. The flora and fauna of the lagoon were formed under the alternating influences of marine transgression or regression stages. The rising abundance and diversity of the marine diatoms in the record provides evidence for marine transgression (warm) stages. The development of freshwater chironomid fauna, decrease or disappearance of marine diatoms, and increase of vegetation characteristic of humid conditions reflect the dominant role of the freshwater input into the lagoon ecosystem and provide evidence for marine regression stages. The Middle Holocene part of the core reflects an open bay or lagoon with shallow overgrown littorals under a strong marine influence. The vegetation of the island corresponded to a warm mixed forest. However, considerable variations in diatom diversity, shifts in dominating taxa, and the sporadic emergence of freshwater chironomids suggest unstable ecological conditions during the late phase of the HCO (6600-4400 cal BP) and changing water levels related to sea level fluctuations and to the intensity of the run-off with the inflowing river. Two short-term declines of marine diatoms, the development of freshwater chironomid fauna, and shifts in vegetation between 6300 and 6100 cal BP and between 5600 and 4400 cal BP can be related to cooling and associated regressions traced also in Japan, on Kunashir, and some other islands. The second one can be correlated with the Neoglacial cooling that occurred at the end of HCO. The period between 4200 and 3200 cal BP was a transition towards the formation of a freshwater lagoon overgrown by macrophytes. This period can be related to a decline of the Late Jomon transgression (Sakaguchi, 1983). Between 3200 and 2800 cal BP (Japan Latest Jomon cold stage) the sea level decrease led to the separation of the lagoon from the marine environment and the formation of the lake ecosystem. The following increase in the share of broad-leaved pollen, especially *Quercus*, indicates a slight warming which can represent Yayoi transition stage, interrupted by a short-term cooling spell between 1500 and 1400 cal BP that can be related to a cold Kofun stage in Japan (ca 1600-1300 cal BP; Sakaguchi, 1983). The shallowing and desiccation of the lake, reflecting a humidity deficit between 1100 and 800 cal BP, can be related to the European Medieval Climate Anomaly (MCA) or relatively dry Japan Nara-Heian-Kamakura warm stage (1200-700 cal BP; Sakaguchi, 1983). The broad spreading of dwarf cedar after 760 cal BP indicates LIA cooling and Edo regression (650-50 cal BP; Sakaguchi, 1983) which caused the swamping of the lake area. Modern warming is not well seen in the investigated core.

Comparison of our newly obtained data from the Iturup Island with the data available from previous studies in the NWP has demonstrated spatial differences in timing and magnitude of the Middle to Late Holocene climatic episodes and strong influence of the local environmental processes including volcanic activities, that played more important than climate role in development of ecosystems. Our results suggest that ecosystem changes in the Southern Kuriles are primarily follow the global and regional climate forcing, however differencies in environmental shifts in different groups of Kuril Islands and their spatial and temporal complexity show that more multi-proxy qualitative and quantitative palaeoecological studies are needed to better document the regional pattern in palaeoclimatic events and to unveil the background mechanisms driving the ecosystems successions in the region.

Author contributions

L. Nazarova conceived and designed research, performed data analysis, N.G. Razjigaeva lead the field work, provided regional data and contributed to analytical work, L.A. Ganzey contributed to landscape

analysis and contributed to analytical work, T.R. Makarova performed diatom analysis, M.S. Lyashevskaya performed pollen analysis, B.K. Biskaborn performed sedimentological analysis and contributed to analytical work, P. Hoelzmann performed geochemical analysis and contributed to analytical work, L.V. Golovatyuk performed chironomid analysis, B. Diekmann contributed to analytical work and overall discussion of the data. All authors wrote, read and approved the manuscript.

Data availability

All data will be lodged with PANGEA upon publication.

Declaration of competing interest

The authors declare that they have no known competing financial interests or personal relationships that could have appeared to influence the work reported in this paper.

Acknowledgements

We thank all Russian colleagues who helped us during the fieldwork. This study was supported by Deutsche Forschungsgemeinschaft (DFG) Project NA 760/5–1 and DI 655/9–1 and within the framework of the state assignment of the TIG FEB RAS (subject, reg. No. AAAA-A19-119030790003-1). The work of L. Golovatyuk was supported by the DAAD (reference nr. 91696266). Our sincere thanks to the anonymous reviewers for their valuable comments.

Appendix A. Supplementary data

Supplementary data to this article can be found online at https://doi.org/10.1016/j.quaint.2021.05.003.

References

Ahn, S.-M., Hwang, J.H., 2015. Temporal fluctuation of human occupation during the 7th–3rd millennium cal BP in the centralwestern Korean Peninsula. Quat. Int. 384, 28–36.

Alberternst, B., Nawrath, S., 2002. Lysichiton americanus newly established in Continental Europe. Is there a chance for control in the early phase of naturalization? NeoBiota 1, 91–99 (in German).

Anderson, L., Abbott, M.B., Finney, B.P., Burns, S.J., 2005. Regional atmospheric circulation in the North Pacific during the Holocene inferred from lacustrine carbonate oxygen isotopes, Yukon Territory, Canada. Qual. Res. 64, 21–35.

Anderson, P.M., Minyuk, P.S., Lozhkin, A.V., Cherepanova, M.V., Borkhodoev, V., Finney, B.A., 2015. Multiproxy record of holocene environmental changes from the northern Kuril islands (Russian Far East). J. Paleolimnol. 54, 379–393.

Anonymous, 2008. China National Analysis Center for Iron and Steel.

Barinova, S.S., Medvedeva, L.A., Anisimova, O.V., 2006. Biodiversity of Algae Indicators of Environment. PiliesStudio, Tel Aviv (in Russian).

Barkalov, V.Yu, 2009. Flora of Kuril Islands. Dalnauka, Vladivostok (in Russian).

Battarbee, R.W., 1986. Diatom analysis. In: Berglund, B.E. (Ed.), Handbook of Holocene Paleoecology and Paleohydrology. Wiley & Sons, London, pp. 527–570.

Bennett, K.D., 1996. Determination of the number of zones in a biostratigraphical sequence. New Phytol. 132, 155–170.

Berner, R.A., Raiswell, R., 1984. C/S method for distinguishing freshwater from marine sedimentary rocks. Geology 12, 365–368.

Birks, H.J.B., Gordon, A.D., 1985. Numerical Methods in Quaternary Pollen Analysis. Academic Press, London.

Biskaborn, B.K., Herzschuh, U., Bolshiyanov, D., Savelieva, L., Diekmann, B., 2012. Environmental variability in northeastern Siberia during the last similar to 13,300 yr inferred from lake diatoms and sediment-geochemical parameters. Palaeogeogr. Palaeoclimatol. Palaeoecol. 329, 22–36.

Biskaborn, B.K., Nazarova, L., Pestryakova, L.A., Syrykh, L., Funck, K., Meyer, H., Chapligin, B., Vyse, S., Gorodnichev, R., Zakharov, E., Wang, R., Schwamborn, G., Bailey, H.L., Diekmann, B., 2019a. Spatial distribution of environmental indicators in surface sediments of Lake Bolshoe Toko, Yakutia, Russia. Biogeosciences 16, 4023–4049.

Biskaborn, B.K., Smith, S.L., Noetzli, J., Matthes, H., Vieira, G., Streletskiy, D.A., Schoeneich, P., Romanovsky, V.E., Lewkowicz, A.G., Abramov, A., Allard, M., Boike, J., Cable, W.L., Christiansen, H.H., Delaloye, R., Diekmann, B., Drozdov, D., Etzelmüller, B., Grosse, G., Guglielmin, M., Ingeman-Nielsen, T., Isaksen, K., Ishikawa, M., Johansson, M., Johannsson, H., Joo, A., Kaverin, D., Kholodov, A., Konstantinov, P., Kröger, T., Lambiel, C., Lanckman, J.-P., Luo, D., Malkova, G., Meiklejohn, I., Moskalenko, N., Oliva, M., Phillips, M., Ramos, M., Sannel, A.B.K., Sergeev, D., Seybold, C., Skryabin, P., Vasiliev, A., Wu, Q., Yoshikawa, K., Zheleznyak, M., Lantuit, H., 2019b. Permafrost is warming at a global scale. Nat. Commun. 10, 264.

Biskaborn, B.K., Subetto, D.A., Savelieva, L.A., Vakhrameeva, P.S., Hansche, A., Herzschuh, U., Klemm, J., Heinecke, L., Pestryakova, L.A., Meyer, H., Kuhn, G., Diekmann, B., 2016. Late Quaternary vegetation and lake system dynamics in north-eastern Siberia: implications for seasonal climate variability. Quat. Sci. Rev. https://doi.org/10.1016/j.quascirev.2015.08.014.

Blaauw, M., Christen, J.A., 2011. Flexible paleoclimate age – depth models using an autoregressive gamma process. Bayesian Anal 6, 457–474.

Bond, G., Showers, W., Cheseby, M., Lotti, R., Almasi, P., Priore, P., Cullen, H., Hajdas, I., Bonani, G., 1997. A pervasive millennial-scale cycle in North Atlantic Holocene and glacial climates. Science 278, 1257–1266.

Brooks, S.J., Diekmann, B., Jones, V.J., Hammarlund, D., 2015. Holocene environmental change in Kamchatka: a synopsis. Global Planet. Change 134, 166–174.

Brooks, S.J., Langdon, P.G., Heiri, O., 2007. The Identification and Use of Palaearctic Chironomidae Larvae in Palaeoecology. QRA Technical Guide No. 10. Quaternary Research Association, London.

Cannings, R.A., Scudder, G.G.E., 1978. The littoral Chironomidae (Diptera) of saline lakes in central British Columbia. Can. J. Zool. 56, 1144–1155.

Chagué-Goff, C., Andrew, A., Szczucinski, W., Goff, J., Nishimura, Y., 2012. Geochemical signatures up to the maximum inundation of the 2011 Tohoku-oki tsunami – implications for the 869 AD Jogan and other palaeotsunamis. Sediment. Geol. 282, 65–77.

Chambers, R.M., Hollibaugh, J.T., Snively, C.S., Plant, J.N., 2000. Iron, sulfur, and carbon diagenesis in sediments of tomales bay, California. Estuaries 23, 1–9.

Chu, G.Q., Sun, Q., Xie, M.M., Lin, Y., Shang, W.Y., Zhu, Q.Z., Shan, Y.B., Xu, D.K., Rioual, P., Wang, L., Liu, J.Q., 2014. Holocene cyclic climatic variations and the role of the Pacific Ocean as recorded in varved sediments from northeastern China. Quat. Sci. Rev. 102, 85–95.

Chéron, S., Etoubleau, J., Bayon, G., Garziglia, S., Boissier, A., 2016. Focus on sulfur count rates along marine sediment cores acquired by XRF Core Scanner. X Ray Spectrom. 45, 288–298.

Davydova, N.N., 1985. Diatoms as Indicators of Holocene Lake Environments. Nauka, Leningrad (in Russian).

deMenocal, P.B., 2001. Cultural responses to climate change during the late holocene. Science 292, 667–673.

Demezhko, D.Yu, Solomina, O.N., 2009. Ground surface temperature change in Kunashir Island inferred from borehole data and tree-ring chronology. Dokl. Akad. Nauk 426, 240–243.

Dixit, Y., Hodell, D.A., Petrie, C.A., 2014. Abrupt weakening of the summer monsoon in northwest Indiă 4100 yr ago. Geology 42, 339–342.

Fallu, M.A., Allaire, N., Pienitz, R., 2000. Freshwater diatoms from northern québec and labrador (Canada). Bibliotheca Diatomologica. Gebr. Borntraeger, Berlin.

Ganzei, K.S., Ivanov, A.N., 2012. Landscape diversity of Kuril islands. Geogr. Nat. Resour. 2, 87–94 (in Russian).

Genkal, S.I., Popovskaya, G.I., Osipov, E.Yu, Onischchuk, N.A., Likhoshway, E.V., 2013. Bacillariophyta in mountainous water bodies of the Barguzin Ridge. Inland. Water Biol. 6, 171–175.

Gleser, Z.I., Jousé, A.P., Makarova, I.V., Proshkina-Lavrenko, A.I., Sheshukova-Poretskaya, V.S. (Eds.), 1974. Diatom Algal of the USSR. Fossil and Modern, vol. 1. Nauka, Leningrad (in Russian).

Gotanda, K., Nakagawa, T., Tarasov, P., Kitagawa, J., Inque, Y., Yasuda, Y., 2002. Biome classification from Japanese pollen data application to modern-day and Late Quaternary samples. Quat. Sci. Rev. 21 (4–6), 647–657.

Gubanov, I.A., Kiseleva, K.V., Novikov, V.S., Tikhomirov, V.N., 2013. Illustrated guide to plants of Central Russia. In: Angiosperms (Dicotyledons: Dicotyledonous), vol. 2. KMK Scientific Publishing Association, Institute of Technological Research, Moscow (in Rissian).

Guiry, M.D., Guiry, G.M., 2019. AlgaeBase. World-wide electronic publication, National University of Ireland, Galway. https://www.algaebase.org.

Harada, N., Katsuki, K., Nakagawa, M., Matsumoto, A., Seki, O., Addison, J.A., Finney, B. P., Sato, M., 2014. Holocene sea surface temperature and sea ice extent in the Okhotsk and Bering Seas. Prog. Oceanogr. 126, 242–253.

Heinecke, L., Mischke, S., Adler, K., Barth, A., Biskaborn, B.K., Plessen, B., Nitze, I., Kuhn, G., Rajabov, I., Herzschuh, U., 2017. Climatic and limnological changes at Lake Karakul (Tajikistan) during the last similar to 29 cal ka. J. Paleolimnol. 58, 317–334.

Heusser, C.J., Igarashi, Y., 1994. Quaternary migration pattern of Selaginella selaginoides in the north pacific. Arctic Antarct. Alpine Res. 26, 187–192.

Hill, M.O., 1973. Diversity and evenness: a unifying notation and its consequences. Ecology 54, 427–432.

Hoelzmann, P., Klein, T., Kutz, F., Schütt, B., 2017. A new device to mount portable energy-dispersive X-ray fluorescence spectrometers (p-ED-XRF) for semi-continuous analyses of split (sediment) cores and solid samples. Geosci. Instrum. Method. Data Syst. 6, 93–101.

Hong, Y.T., Wang, Z.G., Jiang, H.B., Lin, Q.H., Hong, B., Zhu, Y.X., Wang, Y., Xu, L.S., Leng, X.T., Li, H.D., 2001. A 6000-year record of changes in drought and precipitation in northeastern China based on a d13C time series from peat cellulose. Earth Planet Sci. Lett. 185, 111–119.

Hong, Y.T., Hong, B., Lin, Q.H., Shibata, Y., Hirota, M., Zhu, Y.X., Leng, X.T., Wang, Y., Wang, H., Yi, L., 2005. Inverse phase oscillations between the East Asian and Indian Ocean summer monsoons during the last 12 000 years and paleo-El Ni~no. Earth Planet Sci. Lett. 231, 337–346.

Ivanova, G.P., 1990. Scientific and applied handbook on the climate of the USSR. In: Urusov (Ed.), Sakhalin District. Issue, vol. 34. Gidrometeoizdat, Leningrad.
Jo, K., Yi, S., Lee, J.Y., Woo, K.S., Cheng, H., Edwards, L.R., Kim, S.T., 2017. 1000-Year Quasi-Periodicity of weak monsoon events in temperate northeast Asia since the mid-Holocene. Sci. Rep. 7, 15196.
Juggins, S., 2007. C2 Version 1.5 User Guide. Software for Ecological and Palaeoecological Data Analysis and Visualization. Newcastle University, Newcastle upon Tyne, UK.
Kaplin, P.A., Selivanov, A.O., 1999. Sea Level Changes of Russia Seas and Development of the Coasts: Past, Present and Future. GEOS, Moscow (In Russian).
Kawahata, H., Ohshima, H., Shimada, C., Oba, T., 2003. Terrestrial-oceanic environmental change in the southern Okhotsk sea during the holocene. Quat. Int. 108, 67–76.
Khotinsky, N.A., 1977. Holocene of the Northern Eurasia. Nauka, Moscow, p. 200 (in Russian).
Kitagawa, H., Matsumoto, E., 1995. Climatic implications of δ13C variations in a Japanese cedar (Cryptomeria japonica) during the last two millenia. Geophys. Res. Lett. 22, 2155–2158.
Koinig, K., Shotyk, W., Lotter, A., Ohlendorf, C., Sturm, M., 2003. 9000 years of geochemical evolution of lithogenic major and trace elements in the sediment of an alpine lake – the role of climate, vegetation, and land-use history. J. Paleolimnol. 30, 307–320.
Koizumi, I., 1994. Spectral analysis of the diatom paleotemperature records at DSDP sites 579 and 580 near the subarctic front in the western North Pacific. Palaeogeogr. Palaeoclimatol. Palaeoecol. 108, 475–485.
Koizumi, I., Tada, R., Narita, H., Irino, T., Aramaki, T., Oba, T., Yamamoto, H., 2006. Paleoceanographic history around the tsugaru strait between the Japan Sea and the northwest pacific ocean since 30 cal kyr BP. Palaeogeogr. Palaeocl. 232, 36–52.
Komarov, V.L., 1940. Botanical essay of Kamchatka. In: Collected Papers in Kamchatka, vol. 1. The USSR Academy of Science Press, Moscow-Leningrad, pp. 5–52 (In Russian).
Korotky, A.M., Khudyakov, G.I., 1990. Exogenic Geomorphological Systems of Marine Coasts. Nauka, Moscow (in Russian).
Korotky, A.M., Razjigaeva, N.G., Grebennikova, T.A., Ganzey, L.A., Mokhova, L.M., Bazarova, V.B., Sulerzhitsky, L.D., Lutaenko, K.A., 2000. Middle and late-holocene environments and vegetation history of Kunashir island, kurile islands, northwestern pacific. Holocene 10, 311–331.
Korotky, A.M., Razjigaeva, N.G., Grebennikova, T.A., Volkov, V.G., Ganzey, L.A., Bazarova, V.B., 1997. Marine terraces of western Sakhalin island. Catena 30, 61–81.
Korotky, A.M., Volkov, V.G., Grebennikova, T.A., Razzhigaeva, N.G., Pushkar, V.S., Ganzei, L.A., Mokhova, L.M., 2005. Far East. In: Velichko, A.A. (Ed.), Cenozoic Climate and Environmental Changes in Russia, vol. 382. Geol. Soc. Am. Spec., pp. 121–137
Kotlyakov, V.M., Baklanov, P.Ya, Komedchikov, N.N., 2009. Atlas of Kuril Islands. Design-Information-Cartography, Moscow-Vladivostok (in Russian).
Krammer, K., Lange-Bertalot, H., 1986. Bacillariophyceae. Teil 1. Naviculaceae. VEB Gustav Fischer Verlag, Jena.
Krammer, K., Lange-Bertalot, H., 1991. Bacillariophyceae. Teil 3. Centrales, Fragilariaceae, Eunotiaceae. VEB Gustav Fischer Verlag, Jena.
Krasheninnikov, S.P., 1949. The Description of Land Kamchatka. Reprinted from 1755 by the. USSR Academy of Sciences Press, Moscow (in Russian).
Kulakov, A.P., 1973. Quaternary Coastal Lines of Okhotsk and Japan Seas. Nauka, Novosibirsk (in Russian).
Kuprianova, L.A., Alyoshina, L.A., 1972. Pollen and Spores of Plants from European Part of USSR. Nauka, Leningrad (in Russian).
Larocque, I., 2001. How many chironomid head capsules is enough? A statistical approach to determine sample size for paleoclimatic reconstruction. Palaeogeogr. Palaeoclimatol. Palaeoecol. 172, 133–142.
Laverov, N.P., 2005. Modern and Holocene Volcanism in Russia. Nauka, Moscow (in Russian).
Lotter, A.F., Juggins, S., 1991. POLPROF, TRAN and ZONE: programs for plotting, editing and zoning pollen and diatom data. INQUA-Subcommission for the study of the Holocene Working Group on Data-Handling Methods, Newslett. 6, 4–6.
Lozhkin, A.V., Anderson, P.M., Goryachev, N.A., Minyuk, P.S., Pakhomov, A.Yu, Solomatkina, T.B., Cherepanova, M.V., 2010. First lake record of Holocene climate and vegetation changes of the northern Kuril Islands. Dokl. Akad. Nauk. 430, 541–543.
Lozhkin, A., Minyuk, P., Cherepanova, M., Anderson, P., Finney, B., 2017. Holocene environments of central Iturup island, southern Kuril archipelago, Russian Far East. Quat. Res. 88, 23–38.
Lyashchevskaya, M.S., Ganzei, K.S., 2011. Environmental evolution of Iturup island in holocene, kurile islands. Bulletin of Kamchatka regional association ‘‘Educational-Scientific center’’. Earth Sci. 1, 35–45 (in Russian).
Lynch, J., 1990. Provisional elemental values for eight new geochemical lake sediment and stream sediment reference materials LKSD-1, LKSD-2, LKSD-3, LKSD-4, STSD-1, STSD-2, STSD-3 and STSD-4. Geostand. Newsl. 14–1, 153–167.
Maeda, Y., Matsuda, I., Nakada, M., Matsushima, Y., Matsumoto, E., Sato, H., 1994. Holocene sea-level change along the Okhotsk sea in Hokkaido, Japan. Bull. Yamagata Univ. Nat. Sci. 13, 205–229 (in Japanese).
Martyn, D., 1992. Climates of the world. In: Developments in Atmospheric Science, vol. 18. Elsevier, Amsterdam.
Melekestsev, I.V., Braitseva, O.A., Erlikh, E.N., Shantser, A.E., Chelebaeva, A.I., Lupikina, E.G., Egorova, I.A., Kozhemyaka, N.N., 1974. Kamchatka, Kurile and Komandar Islands. History of Developmentof Relief of Siberia and Far East. Nauka, Moscow (in Russian).
Melles, M., Brigham-Grette, J., Minyuk, P.S., Nowaczyk, N.R., Wennrich, V., DeConto, R. M., Anderson, P., Andreev, A.A., Coletti, A., Cook, T., Haltia-Hovi, E., Kukkonen, M., Lozhkin, A.V., Rosén, P., Tarasov, P., Vogel, H., Wagner, B., 2012. 2.8 million years of arctic climate change from Lake El'gygytgyn, NE Russia. Science 337, 315–320.
Meyer, H., Chapligin, B., Hoff, U., Nazarova, L., Diekmann, B., 2015. Oxygen isotope composition of diatoms as late holocene climate proxy at two-yurts-lake, central Kamchatka, Russia. Global Planet. Change 134, 118–128.
Meyers, P.A., Teranes, J.L., 2001. Sediment organic matter. In: Last, W.M., Smol, J.P. (Eds.), Tracking Environmental Change Using Lake Sediments. Physical and Geochemical Methods. Kluwer, Dordrecht, pp. 239–269.
Mikishin, YuA., Gvozdeva, I.G., 1996. The Natural Evolution in the South-Eastern Part of Sakhalin Island in Holocene. FESU Publishing, Vladivostok, p. 130 (in Russian).
Mokhova, L.M., Eremenko, N.A., 2020. Pollen rain composition on Kunashir island (Kuril islands). Biodivers. Environ. Protected Area 2, 3–37 (in Russian with English abstract).
Moller Pillot, H.K.M., 2009. Chironomidae Larvae. Biology and Ecology of the Chironomini. KNNV Publishing. Zeist, The Netherlands.
Moller Pillot, H.K.M., 2013. Chironomidae Larvae. Biology and Ecology of the Aquatic Orthocladiinae. KNNV Publishing, Zeist, The Netherlands.
Nakagawa, M., Ishizuka, Y., Hasegawa, T., Baba, A., Kosugi, A., 2008. Preliminary Report on Volcanological Research of KBP 2007–2008 Cruise by Japanese Volcanology Group. Hokkaido University, Sapporo.
Nazarova, L., Bleibtreu, A., Hoff, U., Dirksen, V., Diekmann, B., 2017a. Changes in temperature and water depth of a small mountain lake during the past 3000 years in Central Kamchatka reflected by chironomid record. Quat. Int. 447, 46–58.
Nazarova, L., de Hoog, V., Hoff, U., Diekmann, B., 2013a. Late Holocene climate and environmental changes in Kamchatka inferred from subfossil chironomid record. Quat. Sci. Rev. 67, 81–92.
Nazarova, L., Grebennikova, T.A., Razjigaeva, N.G., Ganzey, L.A., Belyanina, N.I., Arslanov, K.A., Kaistrenko, V.M., Gorbunov, A.O., Kharlamov, A.A., Rudaya, N., Palagushkina, O., Biskaborn, B.K., Diekmann, B., 2017b. Reconstruction of holocene environmental changes in southern Kurils (North-Western pacific) based on palaeolake sediment proxies from shikotan island. Global Planet. Change 159, 25–36.
Nazarova, L., Herzschuh, U., Wetterich, S., Kumke, T., Pestrjakova, L., 2011. Chironomid-based inference models for estimating mean July air temperature and water depth from lakes in Yakutia, northeastern Russia. J. Paleolimnol. 45, 57–71.
Nazarova, L., Lüpfert, H., Subetto, D., Pestryakova, L., Diekmann, B., 2013b. Holocene climate conditions in Central Yakutia (North-Eastern Siberia) inferred from sediment composition and fossil chironomids of Lake Temje. Quat. Int. 290–291, 264–274.
Nazarova, L.B., Pestryakova, L.A., Ushnitskaya, L.A., Hubberten, H.W., 2008. Chironomids (Diptera: chironomidae) in lakes of Central Yakutia and their indicative potential for paleoclimatic research. Contemp. Probl. Ecol. 1, 335–345.
Nazarova, L.B., Razjigaeva, N.G., Diekmann, B., Grebennikova, T.A., Ganzey, L.A., Belyanina, N.I., Arslanov, K.A., Kaistrenko, V.M., Gorbunov, A.O., Kharlamov, A.A., Golovatyuk, L.V., Syrykh, L.S., Subetto, D.A., Lisitsyn, A.P., 2019. Reconstruction of holocene environmental changes in North-western pacific in relation to paleorecord from shikotan island. Dokl. Earth Sci. 486, 76–80.
Nazarova, L., Self, A., Brooks, S.J., van Hardenbroek, M., Herzschuh, U., Diekmann, B., 2015. Northern Russian chironomid-based modern summer temperature data set and inference models. Global Planet. Change 134, 10–25.
Nazarova, L.B., Self, A.E., Brooks, S.J., Solovieva, N., Syrykh, L.S., Dauvalter, V.A., 2017c. Chironomid fauna of the lakes from the pechora river basin (east of European part of Russian arctic): ecology and reconstruction of recent ecological changes in the region. Contemp. Probl. Ecol. 10, 350–362.
Nazarova, L., Subetto, D., Syrykh, L.S., Grekov, I.M., Leontev, P.A., 2018. Reconstructions of palaeoecological and palaeoclimatic conditions of the Late Pleistocene and Holocene according to the results of chironomid analysis of sediments from Medvedevskoe Lake (Karelian Isthmus). Dokl. Earth Sci. 480, 710–714.
Ota, Y., Matsushima, Y., Moriwaki, H., 1982. Notes on the Holocene sea-level study in Japan – on the basis of ‘Atlas of Holocene sea-level records in Japan’. The Quat. Res. (Daiyonki-Kenkyu) 21, 133–143.
Palagushkina, O.V., Nazarova, L.B., Wetterich, S., Shirrmaister, L., 2012. Diatoms of modern bottom sediments in Siberian Arctic. Contemp. Probl. Ecol. 5, 413–422.
Park, J., Park, J., Yi, S., Kim, J.C., Lee, E., Choi, J., 2019. Abrupt Holocene climate shifts in coastal East Asia, including the 8.2 ka, 4.2 ka, and 2.8 ka BP events, and societal responses on the Korean peninsula. Sci. Rep.-UK. 9, 10806.
Pleskot, K., Tjallingii, R., Makohonienko, M., Nowaczyk, N., Szczucinski, W., 2018. Holocene paleohydrological reconstruction of Lake Strzeszynskie (western Poland) and its implications for the central European climatic transition zone. J. Paleolimnol. 59, 443–459.
Pokrovskaya, I.M., 1966. Methods of paleopollen studies. Nedra, Leningrad. In: Pokrovskaya, I.M. (Ed.), Paleopalinology (in Russian).
Quinlan, R., Smol, J.P., 2001. Setting minimum head capsule abundance and taxa deletion criteria in chironomid-based inference models. J. Paleolimnol. 26, 327342.
R Development Core Team, 2012. R: a Language and Environment for Statistical Computing. R Foundation for Statistical Computing, Vienna, Austria.
Razjigaeva, N.G., Ganzey, L.A., Arslanov, KhA., Grebennikova, T.A., Belyanina, N.I., Mokhova, L.M., 2011. Paleoenvironments of Kuril Islands in Late Pleistocene-Holocene: climatic changes and volcanic eruption effects. Quat. Int. 237, 4–14.
Razjigaeva, N.G., Ganzey, L.A., Bazarova, V.B., Arslanov, KhA., Grebennikova, T.A., Mokhova, L.M., Belyanina, N.I., Lyaschevskaya, M.S., 2019b. Landscape response to the medieval warm period in the south Russian Far East. Quat. Int. 519, 215–231.

Razjigaeva, N.G., Ganzey, L.A., Belyanina, N.I., Grebennikova, T.A., Ganzey, K.S., 2008. Paleo- environments and landscape history of minor Kuril islands since late glacial. Quat. Int. 179, 83–89.
Razjigaeva, N.G., Ganzey, L.A., Grebennikova, T.A., Belyanina, N.I., Ganzei, K.S., Kaistrenko, V.M., Arslanov, KhA., Maksimov, F.E., Rybin, A.V., 2019a. Multiproxy record of late holocene climatic changes and natural hazards from paleolake deposits of Urup Island (Kuril islands). J. Asian Earth Sci. 181, 103916.
Razjigaeva, N.G., Ganzey, L.A., Grebennikova, T.A., Belyanina, N.I., Mokhova, L.M., Arslanov, KhA., Chernov, S.B., 2013. Holocene climatic changes and vegetation development in the Kuril Islands. Quat. Int. 126–138.
Razjigaeva, N.G., Grebennikova, T.A., Ganzey, L.A., Mokhova, L.M., Bazarova, V.B., 2004. The role of global and local factors in determining the middle to late Holocene environmental history of South Kurile and Komandar island, northwestern Pacific: Palaeogeogr. Palaeoclimatol. Palaeoecol. 209, 313–333.
Razjigaeva, N.G., Korotky, A.M., Grebennikova, T.A., Ganzey, L.A., Mokhova, L.M., Bazarova, V.B., Sulerzhitsky, L.D., Lutaenko, K.A., 2002. Holocene climatic changes and environmental history of Iturup island, kurile islands, northwestern pac. Holocene 12, 469–480.
Razzhigaeva, N.G., Matsumoto, A., Nakagawa, M., 2016. Age, source, and distribution of Holocene tephra in the southern Kurile Islands: evaluation of Holocene eruptive eruptive activities in the southern Kurile arc. Quat. Int. 397, 63–78.
Reille, M., 1992. Pollen and Spores from Europe and North Africa. Laboratory of Historical Botany and Palynology. URA CNRS, Marseille, France (in French).
Reille, M., 1995. Pollen and Spores from Europe and North Africa Supplement 1. Laboratory of Historical Botany and Palynology. URA CNRS, Marseille, France (in French).
Reille, M., 1998. Pollen and Spores from Europe and North Africa Supplement 2. Laboratory of Historical Botany and Palynology. URA CNRS, Marseille, France (in French).
Reimer, P.J., Austin, W.E.N., Bard, E., Bayliss, A., Blackwell, P.G., Bronk Ramsey, C., Butzin, M., Cheng, H., Edwards, R.L., Friedrich, M., Grootes, P.M., Guilderson, T.P., Hajdas, I., Heaton, T.J., Hogg, A.G., Hughen, K.A., Kromer, B., Manning, S.W., Muscheler, R., Palmer, J.G., Pearson, C., van der Plicht, J., Reimer, R.W., Richards, D.A., Scott, E.M., Southon, J.R., Turney, C.S.M., Wacker, L., Adolphi, F., Büntgen, U., Capano, M., Fahrni, S.M., Fogtmann-Schulz, A., Friedrich, R., Köhler, P., Kudsk, S., Miyake, F., Olsen, J., Reinig, F., Sakamoto, M., Sookdeo, A., Talamo, S., 2020. The IntCal20 northern hemisphere radiocarbon age calibration curve (0–55 cal kBP). Radiocarbon 62, 725–757.
Saenko, O., Schmittner, A., Weaver, A.J., 2004. The Atlantic-Pacific seasaw. J. Clim. 17, 2033–2038.
Sakaguchi, Y., 1983. Warm and cold stages in the past 7600 years in Japan and their global correlation. Bull. Dep. Geogr. Univ. Tokyo 15, 1–31.
Sakaguchi, Y., Okumura, K., 1986. Interglacial climates and relict red soils in northern Japan based on pollen records of interglacial deposits in Eastern Hokkaido. Bull. Dep. Geogr. Univ. Tokyo 18, 2–48.
Sato, H., Kumano, S., Maeda, Y., Nakamura, T., Matsuda, I., 1998. The holocene development of kushu lake on rebun island in Hokkaido, Japan. J. Paleolimnol. 20, 57–69.
Schleusner, P., Biskaborn, B.K., Kienast, F., Wolter, J., Subetto, D., Diekmann, B., 2014. Basin evolution and palaeoenvironmental variability of the thermokarst lake El'gene-Kyuele. Arct. Sib. Boreas 44, 216–229.
Schwanghart, W., Bernhardt, A., Stolle, A., Hoelzmann, P., Adhikari, B., Andermann, C., Tofelde, S., Merchel, S., Rugel, G., Fort, M., Korup, O., 2016. Repeated catastrophic valley infill following medieval earthquakes in the Nepal Himalaya. Science 351, 147–150.
Seki, O., Meyers, P.A., Kawamura, K., Zheng, Y., Zhou, W., 2009. Hydrogen isotopic ratios of plant wax n-alkanes in a peat bog deposited in northeast China during the last 16 kyr. Org. Geochem. 40, 671–677.
Stebich, M., Rehfeld, K., Schlütz, F., Tarasov, P.E., Liu, J., Mingram, J., 2015. Holocene vegetation and climate dynamics of ne China based on the pollen record from Sihailongwan Maar Lake. Quat. Sci. Rev. 124, 275–289.
Syrykh, L.S., Nazarova, L.B., Herzschuh, U., Subetto, D.A., Grekov, I.M., 2017. Reconstruction of palaeoecological and palaeoclimatic conditions of the Holocene in the south of Taimyr according to the analysis of lake sediments. Contemp. Probl. Ecol. 4, 363–369.
Taira, K., 1980. Environmental changes in Eastern Asia during the past 2000 years. Volcanism, tectonism, climate and palaeooceanology. Palaeogeogr. Palaeoclimatol. Palaeoecol. 32, 89–97.
Taira, K., 1992. Holocene palaeoceanographic changes in Japan. Rep. Taisetsuzan Instit. Sci. 27, 1–7.
Taira, K., Lutaenko, K., 1993. Holocene palaeoceanographic changes in the Sea of Japan. Rep. Taisetsuzan Instit. Sci. 28, 65–70.
ter Braak, C.J.F., Prentice, I.C., 1988. A theory of gradient analysis. Adv. Ecol. Res. 18, 271–317.
ter Braak, C.J.F., Šmilauer, P., 2002. CANOCO Reference Manual and CanoDraw for Windows User's Guide: Software for Canonical Community Ordination (Version 4.5). Microcomp. Power, Ithaca, NY.
Urusov, V.M., Chipizubova, M.N., 2000. Vegetation of Kuriles. Problems of Dynamic and Origin. Dalnauka, Vladivostok (in Russian).
Van Dam, H., Mertens, A., Sinkeldam, J., 1994. A coded checklist and ecological indicator values of freshwater diatoms from The Netherlands. Aquat. Ecol. 28, 117–133.
Velichko, A.A., 2010. Climates and Landscapes of Northern Eurasia Under Conditions of Global Warming. Retrospective Analysis and Scenarios 9–10. GEOS, Moscow (in Russian).
Vorobiev, D.P., 1963. Vegetation of Kuril Islands. USSR Academy of Sciences Publ, Moscow-Leningrad (in Russian).
Vyse, S.A., Herzschuh, U., Andreev, A.A., Pestryakova, L.A., Diekmann, B., Armitage, S. J., Biskaborn, B.K., 2020. Geochemical and sedimentological responses of arctic glacial Lake Ilirney, Chukotka (far east Russia) to palaeoenvironmental change since ~ 51.8 ka BP. Quat. Sci. Rev. 247, 106607.
Wang, Y., Cheng, H., Edwards, R.L., He, Y., Kong, X., An, Z., Wu, J., Kelly, M.J., Dykoski, C.A., Li, X., 2005. The Holocene Asian monsoon: links to solar changes and North Atlantic climate. Science 308, 854–857.
Wang, P.X., Wang, B., Cheng, H., Fasullo, J., Guo, Z.T., Kiefer, T., Liu, Z.Y., 2014. The global monsoon across timescales: coherent variability of regional monsoons. Clim. Past 10, 2007–2052.
Wiederholm, T., 1983. Chironomidae of the holarctic region, keys and diagnoses. Part 1–Larvae: Entomol. Scand. Supplement 19.
Wu, W., Liu, T., 2004. Possible role of the "holocene event 3" on the collapse of neolithic cultures around the central plain of China. Quat. Int. 117, 153–166.
Yasuda, Y., 1995. Climatic changes and the development of Jomon culture in Japan. Proceedings of the VIth International Symposium at the International Research Centre for Japanese Studies. In: Nature and Humankind in the Age of Environmental Crisis, pp. 57–77.
Zhao, J., Tan, L., Yang, Y., Pérez-Mejías, C., Brahim, Y.A., Lan, J., Wang, J., Li, H., Wang, T., Zhang, H., Cheng, H., 2021. New insights towards an integrated understanding of NE Asian monsoon during mid to late Holocene. Quat. Sci. Rev. https://doi.org/10.1016/j.quascirev.2020.106793.
Zheng, Y., Pancost, R.D., Naafs, B.D.A., Li, Q., Liu, Z., Yang, H., 2018. Transition from a warm and dry to a cold and wet climate in NE China across the Holocene. Earth Planet Sci. Lett. 493, 36–46.
Zhou, W., Zheng, Y., Meyers, P.A., Jull, A.J.T., Xie, S., 2010. Postglacial climate-change record in biomarker lipid compositions of the Hani peat sequence, Northeastern China. Earth Planet Sci. Lett. 294, 37–46.